BRIGHAM YOUNG UNIVERSITY

GEOLOGY STUDIES

Volume 18, Part 1 — March 1971

CONTENTS

Brigham Young University Geology Studies

Volume 18, Part 1 — March, 1971

Contents

A publication of the
Department of Geology
Brigham Young University
Provo, Utah 84601

Brigham Young University Geology Studies is published semi-annually by the department. Geology Studies consists of graduate student and staff research in the department and occasional papers from other contributors.

Distributed March 15, 1971

Price $4.00

Petrology and Geochemistry of Shoal Water Carbonates of the Virgin Limestone Member, Triassic Moenkopi Formation Clark County, Nevada*

DENNIS W. BELNAP
Union Oil Company, Durango, Colorado

ABSTRACT.—Five sections of the Virgin Limestone Member of the Triassic Moenkopi Formation measuring at least 20 feet were studied stratigraphically, petrologically, and geochemically. The sections contain two carbonate cycles representative of numerous cycles found in the lower part of the Virgin Limestone in Clark County, Nevada. Carbonate cycles were formed during marine transgression out of the miogeosyncline over the shelf.

Eighty samples were collected from the five study sections; seventy thin sections were prepared, and samples were analyzed for Ca, Mg, Si, Al, K, Na, Fe, and Sr. Data obtained was used to divide the cycles into three parts as follows: a basal transgressive unit, a medial regressive unit containing phylloid algal biocherms, and an upper tidal flat unit composed of cross-bedded terrigenous calcisiltites.

Lateral chemical variations in the basal transgressive unit are useful as indicators of shoreline direction, proximity, and possible means for location of carbonate banks.

CONTENTS

ILLUSTRATIONS

*A thesis submitted to the faculty of the Department of Geology, Brigham Young University, in partial fulfillment o fthe requirements for the degree Master of Science.

INTRODUCTION

The Virgin Limestone Member of the lower Triassic Moenkopi Formation named by Reeside and Bassler (1922) exhibits a classic east to west, shelf to basin transition in southern Nevada. The transition is marked by a major thickening as the Virgin Limestone is traced westward from the craton into the Cordilleran miogeosyncline. Facies variations accentuate the transition and lithologies grading from shales, siltstones, terrigenous limestones, gypstones, and dolostones on the shelf or craton into marine carbonates and shales of the basin or miogeosyncline.

Virgin Limestone beds deposited on the craton crop out a few miles east of the tectonic hinge that segregates the craton from the miogeosyncline. These outcrops present an excellent place to study shelf to basin facies changes on a small scale in a sedimentary realm where the regional depositional patterns are well documented.

The goal of the study was to document the minor petrologic and geochemical facies trends and relationships of two repetitively bedded carbonate suites and delimit the sequence and type of environments that produced the carbonate suites. Furthermore, expected petrologic and geochemical data may prove useful as a tool to predict specific lithologic occurrences and location in the Virgin Limestone or similar carbonate deposits.

Location and Geologic Setting

The base of two carbonate suites studied crops out 180 feet above the base of the Virgin Limestone that forms a spectacular east-west striking, south-dipping hogback (Pl. 1, fig. 1) in Sections 14-16 and 21-23, Township 20 South, Range 65 East in Clark County, Nevada (Text-fig. 1). This hogback is located on the south limb of an east-west striking, doubly-plunging, and faulted anticline that is cored by limestone outcrops of the Permian Toroweap and Kaibab formations. The anticline is located approximately three-tenths of a mile north

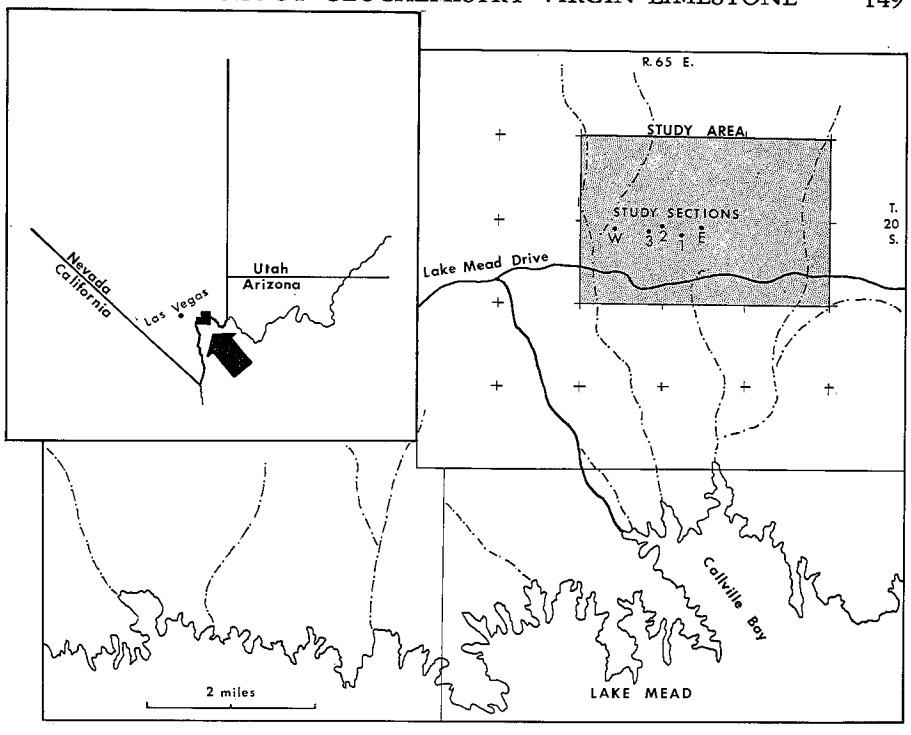

TEXT-FIGURE 1.—Index map showing location of study area and study section.

of Lake Mead Drive in the southwestern part of Bitter Springs Wash, 20 miles east of Henderson, Nevada (Text-fig. 1).

Field Methods

Five study sections were selected at strategically located positions (Text-figs. 1, 4) as determined by amount of exposure, accessibility, and frequency needed to establish adequate lateral lithologic controls. White spray paint was used to mark each location and detailed sampling and measuring was effected. Preliminary field work and thin section studies showed that, to obtain meaningful reproducible, and representative geochemical and petrologic data, samples should be taken from each distinctive bed encountered at each study section.

In order to make geochemical and petrologic data truly indicative of the bed it represents, large samples normally in excess of 10-15 pounds were collected from thin beds. Thick homogeneous beds were sampled at locations empirically selected so that the sample was a microcosm of the bed it represents.

Friable and nonresistant samples were placed in clean plastic bags to avoid contamination, and all samples were taken from locations where contamination from faults, fractures, and weathered surfaces was absent, or at least minimal. Accurate notations as to the thickness of the bed and sample location were recorded.

During sampling, care was taken to observe sedimentary structures, namely ripple marks and cross beds, and other features that would indicate possible cur-

rent and/or transportation direction. Limited, but empirically significant measurements were taken on sedimentary structures encountered. Thus, field work consisted of detailed sampling and measuring at five locations, and measurements and empirical observations related to sedimentary structures and local outcrop relationships of the lithologies.

Laboratory Methods

Petrologic procedure.—Thin sections measuring 2" x 3" were constructed for each resistant sample; they were oriented normal to bedding plane, and care was exercised so that the lithology shown in the thin section was indicative of the lithology in the sample. In all, seventy thin sections were prepared.

All sections were studied under a petrographic microscope. In samples where qualitative textural information was needed, point count analysis and statistical grain measurements were made.

Geochemical procedure.—Samples were analyzed for Ca, Mg, Fe, Si, Mn, Na, K, Sr, and Al because they are the major sedimentary elements whose sedimentary fate is most generally understood. Furthermore their relative abundances can be used to interpret depositional environments.

Samples were prepared for analysis by the following method:

1. 0.50 grams of sample plus two grams of $LiBO_3$ were mixed together in a clean graphite crucible.
2. The crucibles were heated to 1,000° C., and the temperature was maintained until the sample and flux were fused and liquified.
3. The liquid was quenched in flasks containing 450 ml of prepared solution (20 ml of 0.1N NHO_3; 430 ml distilled H_2O).
4. Solutions were then agitated, filtered, and diluted to 1:1,000 and 1:10,000 and placed in appropriately marked nalgene bottles.

Standards were prepared by mixing 0.25, 0.50, 0.75 and 1.00 grams of U.S. Department of Commerce Argillaceous Limestone Standard 2B in four crucibles with appropriated amounts of $LiBO_3$. Standards were then fluxed and quenched like samples to reduce nonrandom errors and diluted to 0.5:1,000, 1.0:1,000, 1.50:1,000, and 2.0:1,000 with distilled H_2O.

The samples were analyzed with a Perkin-Elmer 303 Atomic Absorption spectrophotometer equipped with a strip-chart recorder. Calibrations were made as to specifications outlined by Brimhall and Embree (1970) to obtain optimum results. Machine reponse to concentrations in samples and standards were recorded on the strip-chart recorder. After the run was completed, readings for the known standards were plotted on graph paper and working curve was constructed. Sample readings were then compared to the working curve and abundances were calculated and recorded.

Statistical calculations on control samples show that the data are accurate to 5 percent with 90 percent certainty.

ACKNOWLEDGMENTS

Dr. Harold J. Bissell served as thesis chairman and provided assistance and encouragement in the field, laboratory, and office during the preparation of this thesis, and was always available for consultation. Dr. Willis Brimhall served as

geochemist adviser, and Dr. W. K. Hamblin assisted in photographic work and illustrations as well as providing constructive criticism. Dr. J. Keith Rigby gave of his time and knowledge freely and was a source of advice and counsel.

Wayne Jacobsen and Robert Melton, fellow graduate students, assisted the writer in the field. Forrest Terrell provided assistance during computer work. My wife, Phyllis, was a constant source of patient understanding as well as an excellent thin section technician, draftswoman, and typist.

Union Oil Company of California provided financial support in the form of a Graduate Thesis Assistantship award that made this thesis financially possible.

STRATIGRAPHY AND SEDIMENTATION

Stratigraphy

Regional Stratigraphy.—The Virgin Limestone Member of the Moenkopi Formation is considered to be a shallow water, neritic to tidal flat, marine succession (Bissell, 1968, p. 167) that thickens from a few tens of feet in the grand staircase along the Utah-Arizona border to an excess of 2,345 feet in the Lovell Wash area west of Las Vegas, Nevada (Bissell, 1968).

Major thickening and facies changes take place in the Virgin Limestone as it crosses the Las Vegas Line, a tectonic hinge trending in a southerly direction across Clark County, Nevada. It separates a basin (miogeosyncline) on the west from the shelf (craton) on the east during Permian and early Triassic time (Bissell and Chilingar, 1968).

Clark (1957) noted the thickening and facies changes along the Las Vegas Line but referred to it as the Wasatch Line, and suggested that in no other part of the Great Basin Triassic was the craton (shelf) and the miogeosyncline (basin) known to be in such close proximity. He further stated that the sea oscillated over the hinge line at times, interfingering with terrestrial cratonic beds.

Local Stratigraphy.—The Virgin Limestone is 375 feet thick at the study area, 20 miles east of Las Vegas Line. With respect to Triassic regional sedimentary tectonics, the five study sections form a line normal to basin thickening. Thus, the study sections present an ideal place to study facies changes in an area proximal to the shelf to basin transition of the Virgin Limestone.

Sedimentation.—Virgin Limestone, although generally referred to as a limestone member of the Moenkopi, contains such numerous diverse lithologies that Poborski (1954) proposed elevation of the Moenkopi to group rank and elevation of the Virgin to formation rank, deleting the name "Limestone" and substituting the name "Formation." The writer doesn't agree with Poborkski and feels that the name "Limestone" does apply and is a valid term in southern Nevada.

A lengthy discussion of the nomenclature of the Virgin is not the purpose of this paper, but as will be noted herein, the Virgin is composed of a wide range of lithologic types. A significant factor to remember when considering the lithologies involved is that they are controlled by cyclicity of sedimentation.

Stylolites.—Columnar stylolitic penetration structures occur in most lithologies encountered in the carbonate cycles and inasmuch as their presence may affect the sediment a brief discussion follows. Generally, stylolites were found to be horizontal bedding plane features that in many instances separated constrasting as

well as similar lithologic units (Pl. 2, fig. 2, Pl. 2, fig. 8). However, stylolites were found locally to cross lithologic boundaries and randomly penetrate through a bed, or parallel cross-bed surfaces in oolitic and bioclastic calcarenites.

Originally it was not the purpose of this study to discuss the mode and time of stylolite development, but inasmuch as they are very numerous in the nonterrigenous carbonates and possibly play a significant role in the development of certain lithologies, namely intraclastic calcirudites, and have significant economic bearing, a short discussion follows.

Stylolites in the study area are three-dimensional, tapering interdigitating columns with a clay, iron oxide, organic-rich layer separating the two beds between which the stylolites interdigitate. Certain beds, as can be seen in Pl. 2, fig. 6, have abrupt right-angle lateral terminations and these terminations are always accompanied by stylolitic surfaces. Occasionally stylolites were found in intraclasts with no apparent lateral connection to other stylolites in the matrix material. The size of the stylolites is variable ranging from microstylolites less than one millimeter, to megastylolites with columns in excess of four inches. The following generalities and observations can be made about stylolites found in the study area. They are found in all nonterrigenous carbonate lithologies; they generally parallel the original bedding plane; they are always accompanied by a residual clay, iron oxide, and organic-rich layer; and they always accompany the abrupt lateral termination of beds and are found in intraclasts with no relationship to stylolites in the matrix material. From these observations the writer subscribes to the following pragmatic theory, namely, that stylolites are early diagenetic, pressure solution, penetration features that form while the lithologies involved are within a few feet and possibly even inches of the depositional surface. This theory is supported by the occurrence of stylolites in intraclasts where it was necessary for the stylolites to form prior to brecciation and reincorporation of the clast. In addition the writer believes that the clay, iron oxide, and organic-rich residue that separate the two beds defining the stylolite are the insoluble remains of appreciable quantities of sediments removed by the pressure solution activity allowing the stylolite to form.

Thus stylolites are significant in that they are a means by which much of the sediment deposited could have been redissolved and cycled back into the sea or transported laterally and reprecipitated in accompanying porous facies. Furthermore, as the result of stylolitic formation, the thickness and relative abundance of lithologies in a bed may not reflect the original thickness and/or lithologic abundances. Finally stylolitic formation is possibly a key factor in the development of intraclastic calcirudites as a mechanism for the brecciation of a recently deposited sedimentary layer.

In addition, the stylolitic surface is an excellent avenue for migration of fluids which may be significant in the placement of hydrocarbon reserves.

SEDIMENTATION

Cycles of Deposition

The cyclic nature of the Virgin Limestone has been noted by previous authors. Poborski (1954) discussed cyclic lagoonal sediments in the St. George, Utah area. Lane and Larsen (1964) discussed a 1,780-foot section of Virgin Limestone 45 miles west of Las Vegas, Nevada, in the Lost Cabin Springs area, with respect to its repetitive nature.

Sanderson (1967) made a detailed lithologic and petrologic study in the Blue Diamond Hill area about 20 miles southwest of Las Vegas, Nevada, and made note of the repetitive nature of the Virgin Limestone. He further concluded that the Virgin Triassic seaway was a shallow, neritic realm that, during periods of transgression, deposited oolitic and algal stromatolite units, and during periods of regression, deposited dolomites and algal dolomites.

Cyclic Nomenclature

The following system of cyclic nomenclature is established so that the discussion of cyclicity of sedimentation in the Virgin Limestone may be concise and coherent. A typical carbonate cycle is composed of three Units. In ascending order they are referred to as Unit A,Unit B, and Unit C. The three-part division of the cycle is readily discernible in the outcrop, and laboratory and geochemical experiments redefine and substantiate the tripartite division. To avoid confusion that may arise from misinterpretation of lithologic classifications the writer chose to classify all carbonates according to a modified classification scheme established by M. J. Saunder (1957) (Text-fig. 2).

Unit A.—Unit A is the most resistant ledge-former of the three units. A sharp lithologic break, commonly an uncomfortable surface with an accompanying intraclastic calcirudite, marks the base of Unit A (Pl. 2, fig. 4). The upper

	BIOCLASTIC	OOLITIC	PELLETAL	SKELETAL	INTRACLASTIC	TERRIGENOUS
CALCILUTITE						
CALCISILTITE						
LUTACEOUS CALCARENITE	Fragmental organic remains.	Oolite and coated grains where coating accounts for more than 50% of the grain.	Organically derived pellets and semi-spherical bodies of unknown origin.	Insitu organic remains.	Clastic particles derived from within the Basin.	Clastic particles derived from outside the Basin (Continental).
CALCARENITE						
CALCIRUDITE						
LUTACEOUS CALCIRUDITE						
BIOHERM						
BIOSTROME						

TEXT-FIGURE. 2.—Carbonate classification used during the study, modified from N. J. Sander (1967).

limit of the unit is picked at the bedding plane along which three-dimensional algal bodies composed of articulated phylloid algal plates first occur.

The lithologies comprising Unit A vary with respect to study section, but all lithologic types are classified as normal marine carbonates.

Unit B.—The first occurrence of algal bioherms and the last occurrence of resistant calcilutite beds, when present, mark the base and the top of Unit B respectively. The bioherms of the unit are composed of arched articulated phylloid algal plates (Pl. 1, figs. 3, 4; Pl. 3, fig. 4). Bioherms usually have a flat base with a semicircular outline, in addition all plates are arched around some epicenter of growth. The phylogeny of the algae has not been established but it is similar to the late Paleozoic genus *Archiolithophyllum.*

Bioherms size ranges from 30 feet in diameter to masses smaller than a human fist. It should be noted however that bioherms of different sizes do not as a rule occur together, rather most bioherms at a location are approximately the same size.

Unit C.—Unit C is a nonresistant slope-forming division that is bounded at its base by the top of the last resistant bed of Unit B, and bounded at its top by the unconformity or lithologic break that separates it from Unit A of the superjacent cycle.

Unit C may contain one of two lithologic types or a stratified mixture of both types| The most common lithology in the unit is a cross-bedded terrigenous calcilutite with burrows and cut-and-fill structure. However, a green poorly bedded noncalcareous shale may occur in the upper positions of unit or as is the case in Unit C, Cycle 2 could be the lithologic type in the unit.

Summary.—The Cycles studied vary in thickness at each study section, but average from ten to four feet in thickness; however, thickness of the cycles appears to range from a few feet as in the cycles studied, to cycles in excess of 80 feet thick encountered at the study locality. Cycle studies have been differentiated numerically, and herein will be referred to as Cycle 1 and Cycle 2, with Cycle 2 being the superjacent cycle. During the discussion of the cycles, the westernmost section will be discussed first, with the subsequent Sections 3, 2, 1, and E being discussed in that respective order (Text-fig. 3).

CYCLE 1

Reference is made to Text-fig. 3 for the thicknesses of individual beds discussed in the following section as well as general stratigraphic relationships of Cycle 1.

Section W.—At Section W, Cycle 1 is ten feet thick. Units A, B, and C are 3'4", 3'1", and 3'7" thick respectively.

Unit A contains three beds (W1, W2, W3). The basal one is an intraclastic calcirudite, with rounded elongate intraclasts that parallel the bedding plane in an oolitic, bioclastic matrix (Pl. 4, fig. 4). This calcirudite occurs only in depressions of the erosional contact, thereby defining the base of the cycle (Pl. 2, fig. 4). The overlying bed is an oolitic, bioclastic, and pelletal calcarenite that contains scattered 20 mm by 80 mm horizontally oriented intraclasts. Composition of the intraclasts is similar to that of the matrix (Pl. 3, fig. 7). The uppermost bed of the unit is a calcisiltite with numerous stylolite penetrations (Pl. 4, fig. 7).

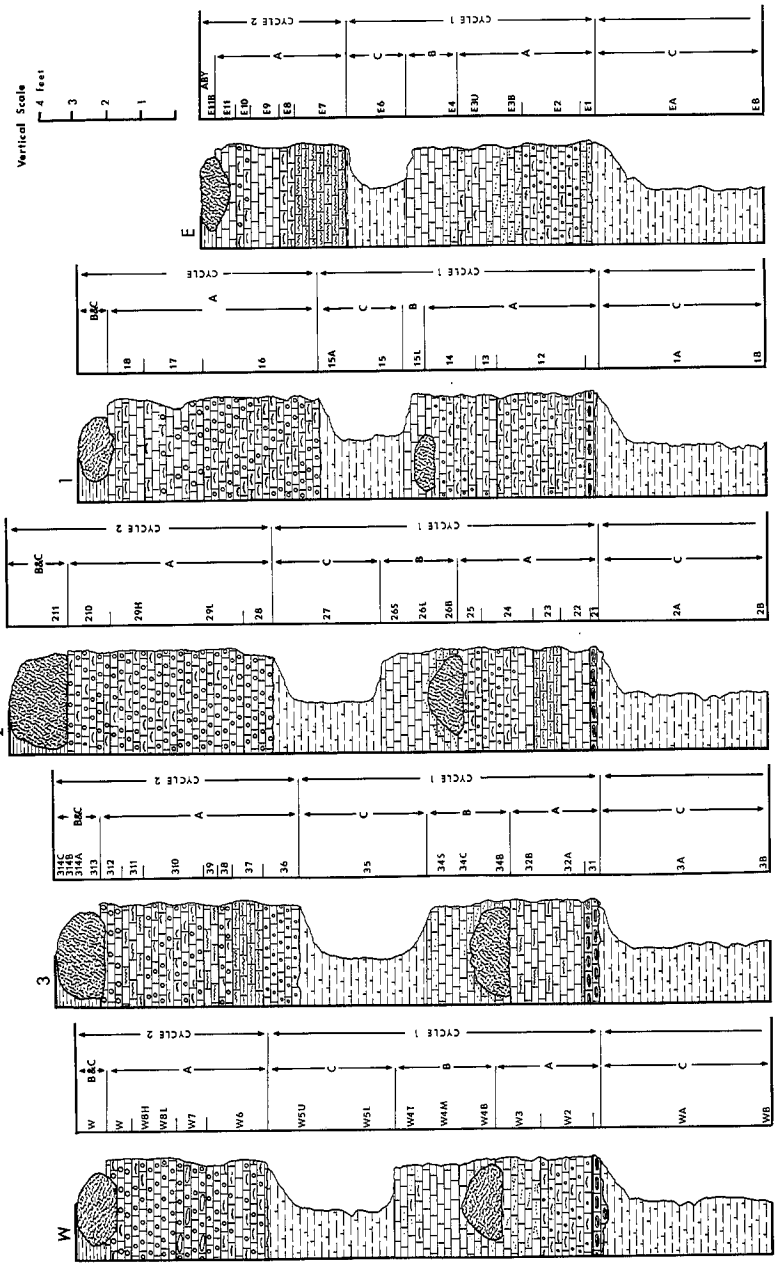

TEXT-FIGURE 3.—Stratigraphic section W through E showing sample locations (for study section location see Text-fig. 4). Sample numbers are explained in text and in appendix.

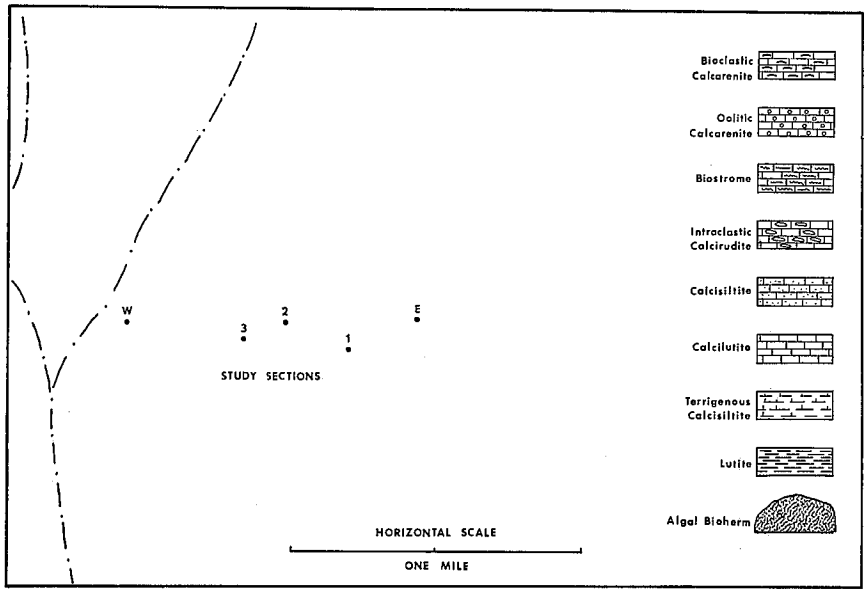

TEXT-FIGURE. 4.—Index map of study sections and legend pertaining to lithologies used in this report.

Algal bioherms (W4B) were the first accumulations in Unit B (Pl. 1, fig. 4; Pl. 2, fig. 7). Subsequently deposited calcisiltites and calcilutites (W4M, W4B), formed beds that drape over and terminate against the flanks of the bioherms (Pl. 2, fig. 7); these average sixteen inches in height, and 30 inches in diameter and depress the substrata four to six inches.

The basal portion of Unit C is composed of a cross-bedded and burrowed terrigenous calcisiltite (Pl. 2, figs. 4, 5) which grades upward into a friable, poorly bedded, green noncalcareous shale (W4T).

Section 3.—At section 3, Cycle 1 is nine feet thick with Units A, B, and C being 2'8", 2'7", and 3'9" thick respectively.

Unit A is composed of two beds, a basal intraclastic calcirudite, (31) (Pl. 4, fig. 4) and an overlying bed consisting of skeletal calcilutites and calcisiltites (Pl. 2, fig. 6; Pl. 4, fig. 7).

Bioherms of Unit B (34B) average 15 inches in height and 30 inches in diameter and are overlain by calcisiltites and calcilutites (34C and 34S) that drape over the bioherm (Pl. 4, fig. 7), but the bioherms do not depress the substrata as in Section W.

The lower half of Unit C is composed of cross-bedded, burrowed, terrigenous calcisiltites (35). The upper portion of Unit C was not sampled because it is seemingly composed of the same lithology that comprises the upper portion of Unit C at Section W.

Section 2.—At Section 2, Units A, B, and C are 4'2", 2'4", and 3'2" thick respectively. The complete cycle is 9'8" thick, eight inches thicker than it is at Section 3, but four inches thinner than at Section W.

Unit A is composed of five beds (21, 22, 23, 24, and 25) and is 13 inches thicker than Unit A at Section 2. The basal calcirudite (Pl. 4, fig. 4) is more uniform in thickness and more widespread at Section 2 because the relief on the erosional surface (Pl. 2, fig 4) is less. Overlying the basal bed is a churned, skeletal calcilutite (Pl. 4, fig. 5) which is overlain by a biostromal layer composed of wavey-laminated leaf-like algal plates (Pl. 4, fig. 3). The fourth bed of the unit is composed of a basal calcilutite that is overlain by layers of progressively coarser lithologic calcarenite (Pl. 4, fig. 2). The uppermost bed of Unit A is an oolitic, bioclastic, pelletal calcarenite (Pl. 3, fig. 1).

The bioherms (26B) of Unit B average 16 inches in height and 30 inches in diameter. Algal plates are scattered throughout the calcilutite and calcisiltite layers (26S, 26L). The highest concentration of algal plates occurs on the eastern side of the bioherms.

Unit C is seven inches thinner than it is at Section 2, and the basal two-thirds of the unit is composed of terrigenous calcisiltites. Again, outcrop limitations prohibited the sampling of the upper portion of Unit C.

Section 1.—A marked change in the relative thickness of the units has taken place between Section 2 and Section 1. At Section 1, Units A, B, and C are 5'1", nine inches, and 2'7" thick respectively.

Unit A is composed of four beds (11, 12, 13, 14). The basal intraclastic calcirudite is present and widespread as at Section 2 and the erosional surface is poorly defined. It is overlain by a cross-bedded, oolitic, and bioclastic pelletal lutaceous calcarenite (Pl. 3, fig. 1). Cross-beds dip to the east; the average height of each set is ten inches. The overlying bed (13) is composed of interbedded calcilutites, calcisiltites, and bioclastic, oolitic calcarenites (Pl. 4, fig. 2). The uppermost bed of Unit A is an oolitic, bioclastic, pelletal, lutaceous calcarenite in which the coated and rounded bioclasts are horizontally oriented.

Algal bioherms of Unit B are small, averaging eight inches in height and 16 inches in width; they depress the substrata four to five inches. Bioherms occur at widely spaced intervals with as much as 80 feet separating individual growths. Calcisiltite which surrounds the bioherms and comprises most of the unit is thoroughly churned and displays numerous desiccation structures.

Unit C is seven inches thinner than at Section 2 and is composed of the same burrowed, cross-bedded, terrigenous calcisiltite (15 and 15A).

Section E.—At the easternmost study section, Cycle 1 is 8'4" thick. Algal bioherms, which are the criterion upon which Units A and B are differentiated, are absent, and geochemical parameters were used to define Unit B. Units A, B, and C are 4'1", 1'7", and one foot thick respectively. The basal calcarenite found at Sections W through 1 is absent at Section E. The basal bed is a laminated calcisiltite. An erosional contact is poorly defined and when traced farther east is not recognizable as such. The overlying bed (E2) is an oolitic, pelletal, bioclastic, lutaceous calcarenite. Coated and rounded bioclasts of the bed are horizontally oriented. The uppermost bed of Unit A was sampled twice (3EB, 3EU) and is shown to be composed of a calcilutite at its base that grades upward into a highly churned, skeletal calcilutite (Pl. 4, fig. 5).

Unit B contains no bioherms and is composed of a laminated calcisiltite at the base which grades upward into a laminated calcilutite.

Unit C is ten inches thinner at Section E than at Section 1, and is composed of a similar cross-bedded, burrowed, terrigenous calcisiltite (Pl. 2, fig. 4).

EXPLANATION OF PLATE 1

OUTCROPS AND SEDIMENTARY FEATURES

FIG. 1.—Virgin hogback dipping south, arrow shows location of study Section 2.
FIG. 2.—Crossbedded oolitic bioclastic calcarenite dipping east to study Section 2.
FIG. 3.—Algal bioherm of Cycle 2 at study Section 2.
FIG. 4.—Algal bioherm of Cycle 1 at study Section 2.

EXPLANATION OF PLATE 2

SEDIMENTARY FEATURES

FIG. 1.—Calcirudite of Unit A, Cycle 2 at study Section W.
FIG. 2.—Ripple marked surface of Unit A, Cycle 2 at study Section 2.
FIG. 3.—Windrows of algae of Cycle 1 east of study Section 2.
FIG. 4.—Erosional contact between cycles at study Section 2 but serves as example for basal contact of Cycle 1 throughout the study area.
FIG. 7.—Algal bioherm surrounded by calcilutites in Cycle 1 at location 2.
FIG. 8.—Photomicrograph of stylolitic penetration (X10).

EXPLANATION OF PLATE 3

PHOTOMICROGRAPHS

(all X3)

FIG. 1.—Oolitic, pelletal, bioclastic calcarenite common in Unit A, Cycle 1.
FIG. 2.—Oolitic pelletal bioclastic lutaceous calcarenite, often crossbedded, common in Unit A, Cycle. 2.
FIG. 3.—Coarse grained, recrystallized, oolitic, bioclastic lutaceous calcarenite, most common in western section in Unit A, Cycle 2.
FIG. 4.—Section of an algal bioherm showing the arched articulated phylloid plates.
FIG. 5.—Cross-bedded oolitic bioclastic calcarenite (see Pl. 1, fig. 2), most bioclastic particles are algal plates.
FIG. 6.—Oolitic lutaceous calcarenite, from the base portion of Unit A, Cycle 2, study Section 2.
FIG. 7.—Calcirudite from Bed W7, matrix is a fine grained oolitic pelletal bioclastic calcarenite.
FIG. 8.—Coarse grained oolitic bioclastic lutaceous calcarenite generally found just subjacent to algal bioherms.

EXPLANATION OF PLATE 4

PHOTOMICROGRAPHS

(all X3)

FIG. 1.—Calcirudite common in western sections.
FIG. 2.—Stylolitic structures at base of calcisiltite which grade upward into a bioclastic lutaceous calcarenite.
FIG. 3.—Biostromal algae common in study Section 3 and E.
FIG. 4.—Base calcirudite matrix is primarily of algal bioclasts.
FIG. 5.—Churned calcilutite with scattered bioclasts and oolites common in eastern section of Unit A, Cycle 1.
FIG. 6.—Calcilutite bed separated from calcilutite by stylolite near the base.
FIG. 7.—Calcilutite showing various amounts of recrystallization with numerous stylolites and bioturbation; this lithology is common in the beds that surround the algal bioherms of Cycle 1.
FIG. 8.—Algal plate of a biostromal bed.

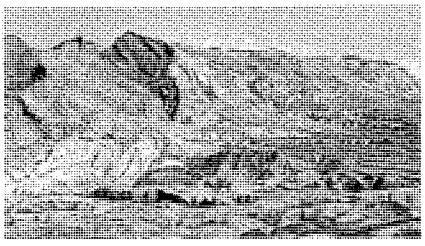

1

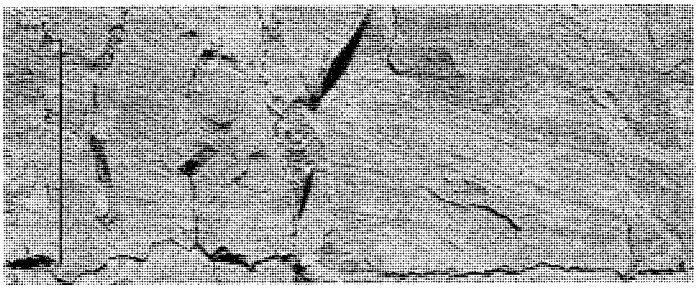

2

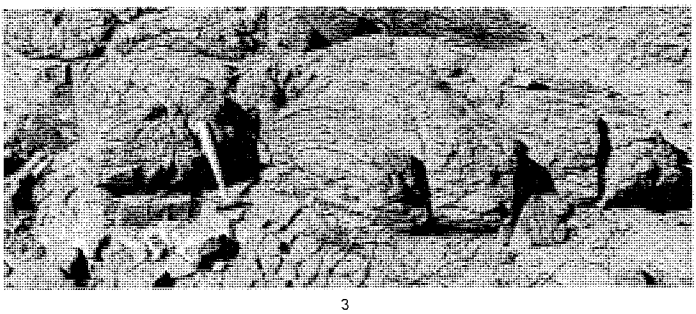

3

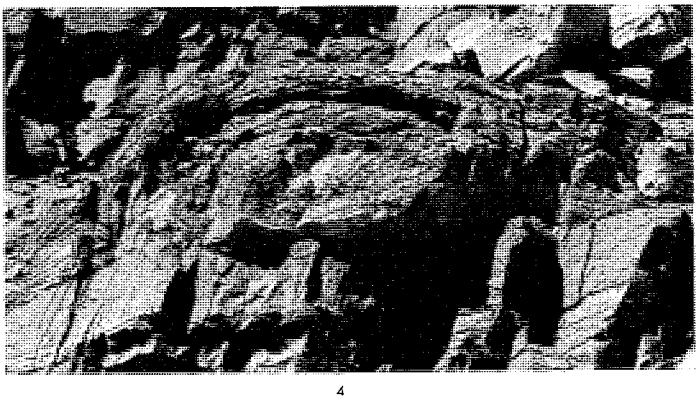

4

PLATE 1

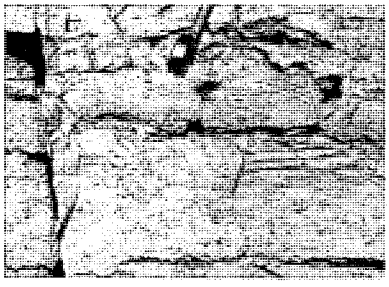

1

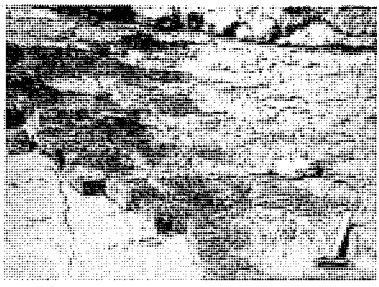

2

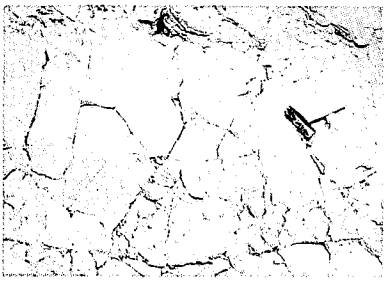

3

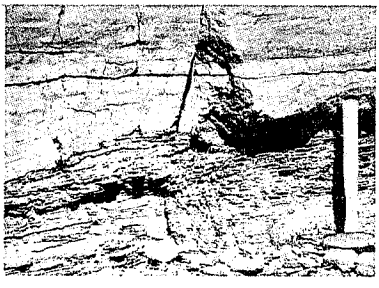

4

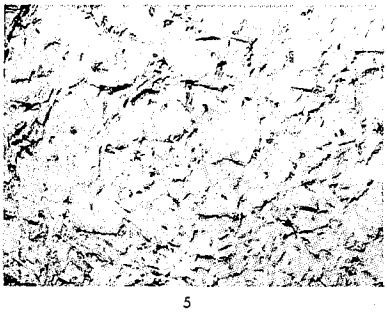

5

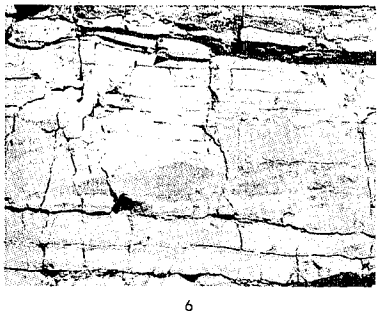

6

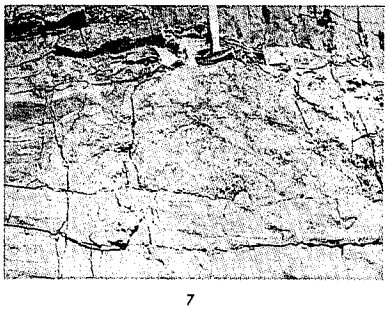

7

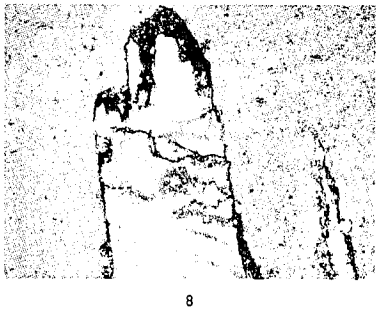

8

PLATE 2

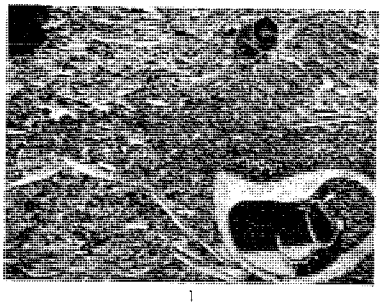

1

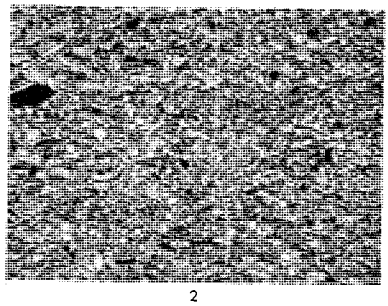

2

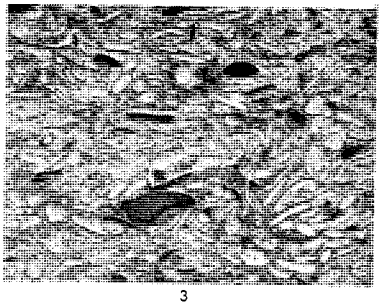

3

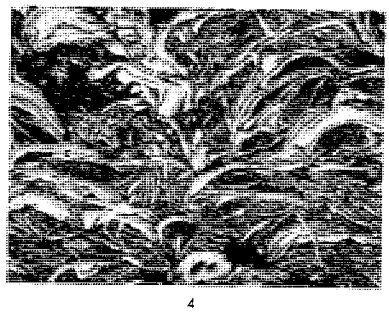

4

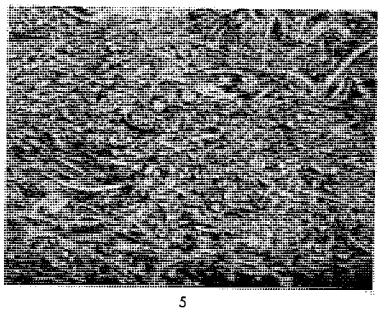

5

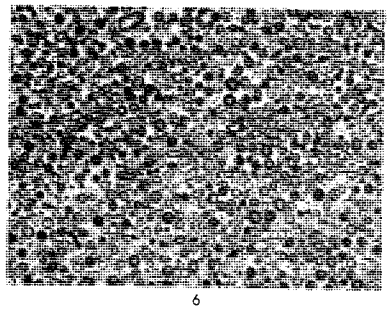

6

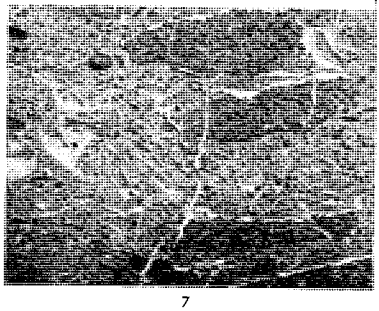

7

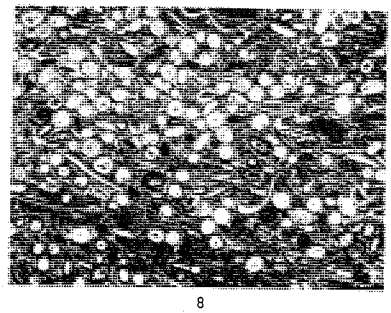

8

PLATE 3

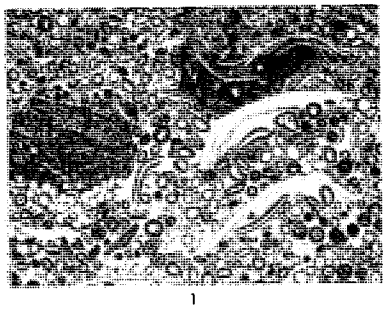

1

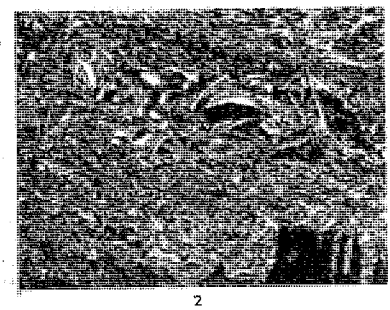

2

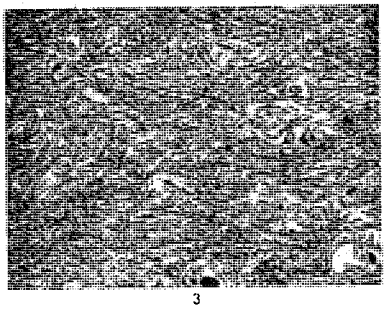

3

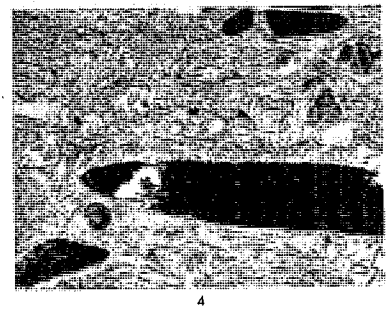

4

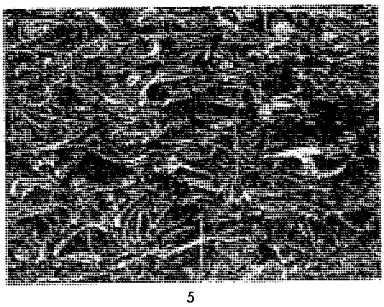

5

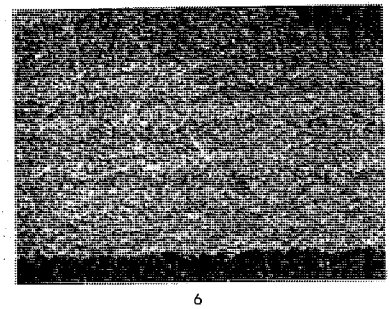

6

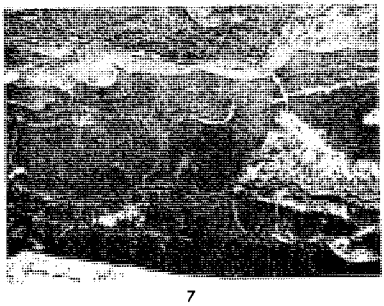

7

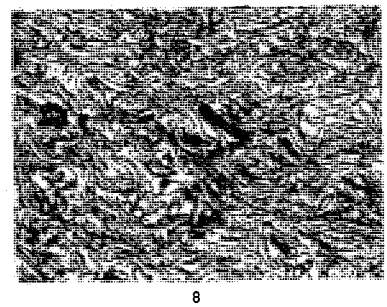

8

PLATE 4

CYCLE 2

Cycle 2 differs from Cycle 1 in that the essential components of Unit B are algal bioherms. Calcilutites and calcisiltites that drape over and terminate against bioherms in Unit B of Cycle 1 are absent in Cycle 2. Thus, Unit C lies in direct contact with Unit A except where bioherms separate the two units. Furthermore, an erosional contact which defines the base of Cycle 2 is poorly defined, and a basal intraclastic calcirudite common in Cycle 1 is absent at the base of Cycle 2.

Section W.—Cycle 2 is 5'8" thick at Section W. Unit A is 4'9" thick, and Unit C is 11 inches thick.

Unit A is composed of four beds (W6, W7, W8, W9), the basal of which is a cross-bedded, oolitic, bioclastic, pelletal, and skeletal lutaceous calcarenite. Cross-beds dip to the east and the maximum height of any cross-bed set is eight inches. Oolites of the bed have a bimodal size distribution with the larger fraction averaging 0.41 mm in diameter with the smaller fraction overaging 0.13 mm in diameter.

The overlying bed is an intraclastic, calrudite with an oolitic, pelletal bioclastic matrix (Pl. 2, fig. 2; Pl. 3, fig. 7). Intraclasts average one and one-half inch in diameter, and are horizontally oriented. Stylolitic structures frequently bound the intraclasts, but are absent in the matrix. This phenomenon suggests that the stylolitic structures developed prior to the incorporation of the intraclasts and were possibly mechanisms of brecciation that produced the intraclasts.

The third bed (W8) of Unit A is a coarse-grained, oolitic, bioclastic, pelletal calcarenite (Pl. 3, fig. 3). Measurements show that the average oolite is 0.61 mm in diameter.

An uppermost bed is oolitic, bioclastic, pelletal calcarenite with scattered oolitic, lutaceous calcarenite intraclasts (Pl. 4, fig. 4). Average diameter of oolites in the bed is 0.69 mm.

Algal bioherms of Unit B average 14 inches in height and 24 inches in diameter, and are depressed into Unit A four to six inches depending upon the size of the bioherms. The smallest bioherms are depressed the most into the substrata. Because the unit was covered extensively with slope talus, Unit C was not sampled.

Section 3.—Cycle 1 is 7'2" thick at Section 3 with Units A and C 6'10", and one foot thick respectively.

The basal bed of Unit A (36) is a well-sorted, oolitic, lutaceous calcarenite (Pl. 3, fig. 6). The overlying bed (37) is an algal biostrome (Pl. 4, fig. 3) which is overlain by an oolitic, pelletal, bioclastic calcarenite (38) which contains oriented bioclastic particles (Pl. 4, fig. 8). Bed (39) is a skeletal, calcilutite which is overlain by a cross-bedded, oolitic, bioclastic, pelletal calcarenite (Pl. 3, fig. 7). Cross-beds of the unit dip to the east. The overlying bed (311) is an algal biostrome which is overlain by the uppermost bed of Unit A, here consisting of a coarse-grained, oolitic, bioclastic calcarenite (Pl. 3, fig. 5).

Algal bioherms (313), the sole components of unit 8 in cycle 1, average 16 inches to two feet in height and eight feet to 12 feet in diameter. Although the bioherms have proportionally larger dimensions, they depress the substrata less than the smaller bioherms at Section W.

Unit C was sampled at three horizons (314A, 314B, 314C) and was found to be a calcareous green shale at the base of the unit which grades upward into a noncalcareous green shale.

Section 2.—Cycle 1 is eight feet thick at Section 2, ten inches thicker than at Section 3. Units A and C are six feet and two feet thick respectively.

Unit A is composed of three beds (28, 29L, 29H, 21O), the basal of which is composed of a well-sorted oolitic, lutaceous calcarenite (Pl. 3, fig. 5) being very similar to bed 36 at Section 3. It is overlain by a cross-bedded oolitic, bioclastic calcarenite (Pl. 1, fig. 2, Pl. 3, fig. 5). Maximum height of the cross-bed sets is 3'10", and all sets dip to the east. The uppermost bed of Unit A at Section 2 (210) is almost identical to bed (312) of Section 3 (Pl. 3, fig. 8).

Unit B at Section 2 is composed of the largest bioherms found in any cycle in the study area. Bioherms average two feet to 2'8" in height and range from ten feet to 25 feet in diameter (Pl. 1, fig. 3); however, the depression of the substrata by the largest bioherms is less than the depression of the smallest bioherms encountered.

Unit C was not sampled at Section 2 because the unit is so non-resistant the wash prohibited sampling.

Section 1.—Cycle 2 is 7'3" thick at Section 1, where Unit A is 6'3" thick. Thickness of Unit C at Section 1 does not exceed two feet.

Unit A is composed of three beds (16, 17, 18). The basal (16) is a cross-bedded, oolitic, bioclastic calcarenite with cross-bed sets dipping east, and a maximum cross-bed height of 3'6". Without doubt, this bed correlates with Bed 29 at Section 2.

The basal portion of the overlying bed is an oolitic, bioclastic calcarenite. It grades upward into a churned calcilutite (Pl. 4, fig. 5), and the uppermost bed of the unit (18) is composed of interbedded calcisiltites and bioclastic, skeletal calcarenites.

Algal bioherms of Unit B are one foot in height and two feet in diameter, depressing the substrata four to five inches.

Section E.—Cycle 1 thins substantially between Section 1 and Section E. At Section E the cycle is 4'3" thick, three feet thinner than it is at Section 1. Unit A is 3'9" thick, and Unit C is six inches thick.

Unit A is composed of five beds (E7, E8, E9, E10, E11) which, when compared to Sections W through 1, display a marked lack of oolitic and bioclastic grains. The basal bed of Unit A (37) is an algal biostrome (Pl. 4, fig. 3) which is overlain by a pelletal, bioclastic calcarenite bed. The overlying bed (E9) is a calcisiltite which is overlain by bed E10, an oolitic, lutaceous calcarenite (Pl. 3, fig. 8).

The uppermost bed of Unit A is a skeletal calcilutite upon which the bioherms (E11) rest. Bioherms average one foot in height and 30 inches in diameter, and are depressed as much as six inches into the substrata.

Unit C was sampled at Section 1 and is shown to be a bed of calcareous green shale.

Summary.—A positive correlation exists between the thickness of Units A and the mean grain percent of the units (Text-fig. 5). Furthermore, all sets of major cross-beds dip to the east (Pl. 1, fig. 2), and the coarsest grained carbonates

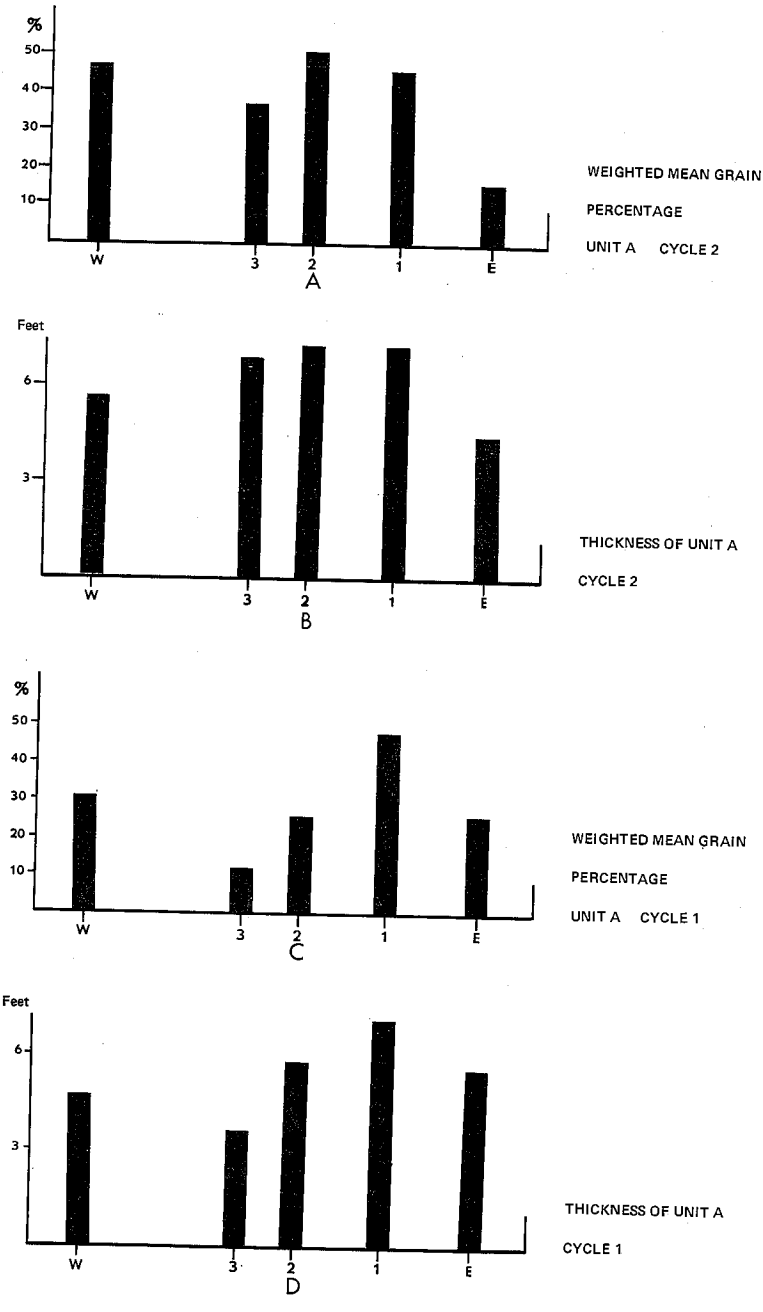

TEXT-FIGURE 5.—Histograms A, B, C, and D showing thickness and weighted mean grain percent for Units A, Cycles 1 and 2.

in Units A occur in the western sections and the unit becomes more lutaceous in the eastern near-shore sections (Text-fig. 3).

This data synthesized with interpretations of regional deposition patterns support the interpretation that Units A of Virgin Carbonate cycles are shoal water marine banks. The banks are produced during periods of west to east marine transgression with marine currents, tides, and possibly wave actions winnowing and depositing oolites, bioclasts, and pellets in banks that parallel the shore and are somewhat comparable to modern banks described by Newell and Rigby (1951) near Andros Island.

It is further interpreted that during the waning stage of west to east marine transgressions or during the early stages of regression, water energy decreased. At that time phylloid algae started to grow on the banks and formed the bioherms that characterize Unit B. This interpretation is supported by the fact that the bioherms are surrounded by fine grained carbonates (Text-fig. 3). In addition the fine-grained carbonates contain desiccation structures which are interpreted to mean that not only was here a decrease in water energy but also a decrease in water depth during the deposition of units B in the regressive Triassic seas.

The size and frequency of occurrence of algal bioherms in Unit B appears to be due to two factors, proximity to the strandline and the thickness and grain percentage of the subjacent unit. A progressive decrease in bioherm size can be noted in Cycle 1 from west to east (Text-fig. 3) as the strandline is approached. The trend is modified in Cycle 2 in that the largest bioherms occur over the thickest part of Unit A which has the greatest grain percentage (Text-figs. 3, 5, 12). Further observation of the bioherms in Cycle 2 reveals that the largest bioherms depress the substrata the least while smaller bioherms cause the greatest depression of the substrata. Thus, it is concluded that the growth of the algal communities was the greatest on carbonate banks removed from the near-shore turbidity, and algal growth was stunted in near-shore turbid water. However, the potential size of the bioherms was proportional to the support offered by the underlying bank carbonates of Unit A.

The contact between the calcilutites and calcisiltites of Units B and the terrigenous calcisiltites and green shales of Units C is gradational. This fact is interpreted to indicate that the seas continued to regress and the shallow marine environment that prevailed during the deposition of Unit B was supplanted by a tidal flat environment that characterized the region during deposition of Unit C.

GEOCHEMISTRY

General Statement

Sedimentary differentiation during weathering and transportation leads to the geochemical differentiation of the major sedimentary elements. They are deposited as sedimentary fractions, geochemically classified by Mason (1955) as follows: 1) resistates, which are composed mostly of quartz with minor resistant constituents such as zircon and magnetite; 2) hydrolysates, composed mostly of clay minerals and adhering ions such as potassium; 3) oxidates, principally oxides of iron and manganese; 4) carbonates, composed chiefly of $CaCO_3$ but containing Mg, Fe, Sr, and other elements in the carbonate mineral, and evaporites which are quantitatively insignificant but geologically and environmentally important.

Transportation distances, water depth and salinity, oxidation-reduction potential, and biologic action are some of the complex and interacting factors affecting the geochemical sedimentary type into which elements are incorporated. For example, iron may occur in a sedimentary rock as an oxide, an ion in a carbonate or hydrolysate, or as an ion in the lattice of a resistate detrital grain. The mode of occurrence of an element is as important as the bulk accumulation.

The discussion will be divided into five parts, which represent the five geochemical fractions of the sedimentary rocks. Elements will be discussed with the geochemical type that incorporates them into the sediments as follows: 1) resistates incorporate for the most part Si; 2) hydrolysates incorporate Al, Si, K and possibly Na and Fe; 3) oxidates incorporate Fe and Mn; 4) carbonates concentrate Ca, Mg, Sr, Fe, and Mn; 5) evaporates incorporate Na, Mg, and Ca.

In the absence of mineralogical data, however, the true significance of elemental associations and variations is often obscured, except where complement-

TABLE 1
WEIGHTED MEAN ELEMENTAL OXIDE ABUNDANCE FOR ALL UNITS OF CYCLE 1 AND 2 AT ALL STUDY SECTIONS (W THROUGH E)

UNITS SECTIONS	SiO_2	Al_2O_3	Fe_2O_3	MnO	CaO	SrO	MgO	Na_2O	K_2O
CYCLE 1									
UNIT A	3.42	0.64	0.57	0.030	49.45	0.151	0.50	0.013	0.222
Sec. E	3.39	0.67	0.59	0.024	44.30	0.179	0.48	0.012	0.189
Sec. 1	3.08	0.58	0.59	0.033	55.44	0.113	0.46	0.012	0.173
Sec. 2	2.86	0.59	0.68	0.032	49.68	0.116	0.47	0.010	0.208
Sec. 3	5.31	0.96	0.55	0.033	45.34	0.193	0.56	0.018	0.416
Sec. W	2.43	0.40	0.49	0.031	52.50	0.153	0.55	0.013	0.126
UNIT B	7.14	1.55	0.81	0.037	39.60	0.247	1.45	0.022	0.526
Sec. E	6.67	1.58	0.74	0.032	40.83	0.148	1.68	0.019	0.541
Sec. 1	7.15	1.49	0.59	0.042	39.45	0.092	1.06	0.023	0.281
Sec. 2	8.49	1.76	0.91	0.036	36.70	0.146	1.96	0.021	0.654
Sec. 3	6.93	1.47	1.02	0.034	41.41	0.135	1.29	0.023	0.563
Sec. W	6.44	1.45	0.81	0.044	39.60	0.714	1.27	0.023	0.592
UNIT C	14.00	3.42	1.77	0.039	19.45	0.071	2.06	0.052	2.216
Sec. E	12.58	2.87	1.23	0.036	21.25	0.085	2.12	0.054	1.370
Sec. 1	12.60	2.85	1.02	0.044	21.25	0.070	1.15	0.041	1.394
Sec. 2	9.44	1.98	2.19	0.041	31.50	0.110	1.42	0.031	0.864
Sec. 3	14.28	3.50	1.72	0.040	16.50	0.060	1.95	0.065	1.570
Sec. W	21.10	5.91	2.67	0.035	6.79	0.030	3.28	0.068	5.884
CYCLE 2									
UNIT A	3.77	0.92	0.63	0.030	47.48	0.339	0.63	0.017	0.313
Sec. E	5.35	1.23	0.66	0.034	45.55	0.160	0.76	0.017	0.553
Sec. 1	3.95	0.97	0.74	0.031	46.27	0.188	0.58	0.016	0.278
Sec. 2	3.25	0.83	0.43	0.026	48.40	0.382	0.55	0.016	0.257
Sec. 3	3.70	0.93	0.64	0.031	46.13	0.460	0.60	0.018	0.281
Sec. W	2.67	0.62	0.69	0.030	51.09	0.505	0.70	0.017	0.194
UNIT B	8.59	1.56	0.93	0.049	36.00	0.134	1.12	0.024	0.520
Sec. E	10.09	1.74	1.16	0.047	30.75	0.120	1.15	0.025	0.745
Sec. 1	NS*	NS	NS	NS	NS	NS	NS	NS	NS
Sec. 2	7.85	1.57	0.92	0.050	39.50	0.185	1.05	0.021	0.435
Sec. 3	8.15	1.47	0.81	0.058	37.13	0.105	0.90	0.020	0.467
Sec. W	8.25	1.46	0.85	0.040	36.63	0.125	1.05	0.032	0.434
UNIT C	22.34	6.89	3.12	0.038	3.43	0.033	3.86	0.067	5.581
Sec. E	23.04	7.43	3.31	0.035	1.00	0.026	5.20	0.074	6.060
Sec. 1	NS	NS	NS	NS	NS	NS	NS	NS	NS
Sec. 2	NS	NS	NS	NS	NS	NS	NS	NS	NS
Sec. 3	21.64	6.35	2.93	0.041	5.92	0.046	2.53	0.061	5.109
Sec. W	NS	NS	NS	NS	NS	NS	NS	NS	NS

* Not Sampled

ing petrologic data and consistent chemical associations make the conclusions reached reliable. Mineralogical data were not derived because they were beyond the scope of the study, but they would be a significant addition to the study, as would analysis for Ba and Rb. Both could be facilitated inasmuch as all samples are curated at Brigham Young University.

The amounts of various elements were calculated and recorded as oxide percentages as in the Illinois State Geological Survey Circular 301 (1960). During the discussion when the amount of an element is said to increase or decrease, it does inasmuch as the oxide increases. The data and all elemental amounts, ratios, and weighted mean percentages of the unit are found in Appendix 1. The precision of the analyses as mentioned in the introduction is ± 5 percent with 90 percent certainty.

Carbonates

The Virgin Limestone in the study area has long been recognized as a carbonate realm. Thus it comes as no surprise that the most abundant element in most samples is calcium. Calcium and magnesium are listed as the major elements of carbonates by Mason (1955) with iron, strontium, and manganese substituting in the calcite and aragonite.

Inasmuch as potassium is representative of relative hydrolysate concentration and calcium a reflection of total carbonate concentraion, calcium and potassium quantities were plotted on the same graph (Text-fig. 6). The plot demonstrates the striking negative correlation between CaO and hydrolysates and accentuates the rhythmic pattern of sedimentation with CaO content greatest in Unit A, and Units B and C containing progressively less CaO (Table 1).

Calcium's relationship with magnesium is striking, and a comparison of Text-figures 6 and 7 shows a strong negative relationship between calcium and magnesium. This relationship may be interpreted to mean that magnesium is incorporated in the sediments as an ion that adheres to hydrolysates. A close inspection of Text-figures 7 and 8, however, shows that magnesium does not accompany aluminum and silicon as precisely as does potassium and sodium. Therefore, it is believed that magnesium's correlation to hydrolysates is due to some environmental change that selectively incoroporates more magnesium in the carbonate fraction as the carbonate fraction was diluted by hydrolysates.

Chilingar (1955) and Siegel (1961) suggest that temperature is the primary control of magnesium content, other investigations that suggest a relationship between evaporation and a high magnesium content add credence to the paleotemperature significance of magnesium contents. Application of this data to the cycles would suggest that the temperature of the water in the Triassic sea in the study area was the coolest during the deposition of Unit A with progressively warmer temperatures prevailing during the formation of Units B and C.

The relationship of Fe_2O_3 to the carbonate fraction is not as clear or intelligible as that of magnesium. However, the radius of Fe^{+2} ion is such that some substitution of iron in the calcite lattice during deposition of the high magnesium calcites could be possible.

Strontium shows a negative correlation to all elements in vertical facies changes but shows a marked increase from east to west in Unit A. A summary of relevant literature (Odium, 1950, Lowenstan 1954, Turkanian 1955, and Pilkey and Howard 1960) reveals that definitive environmental predictions based on strontium content are alone questionable, but SrO/MgO and SrO/CaO

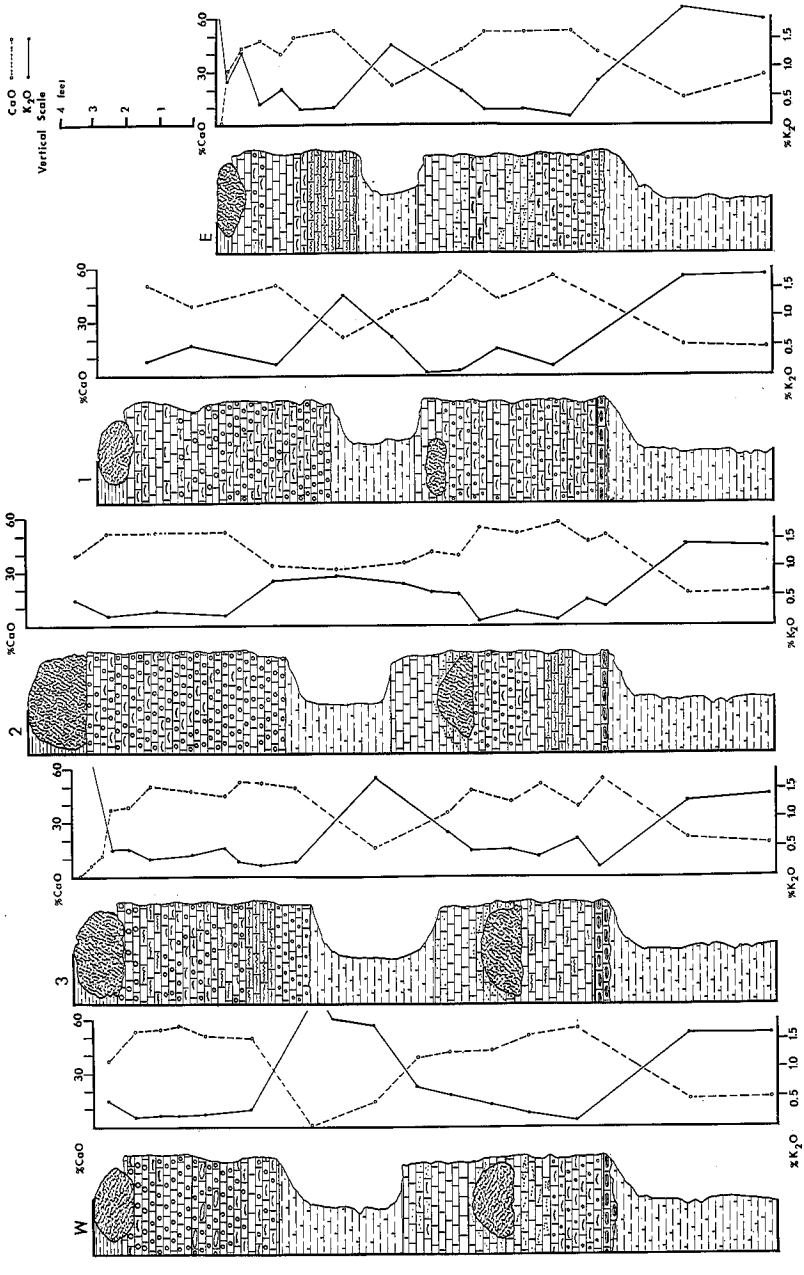

TEXT-FIGURE 6.—CaO (dashed) and K_2O (solid) percentage plots for study sections.

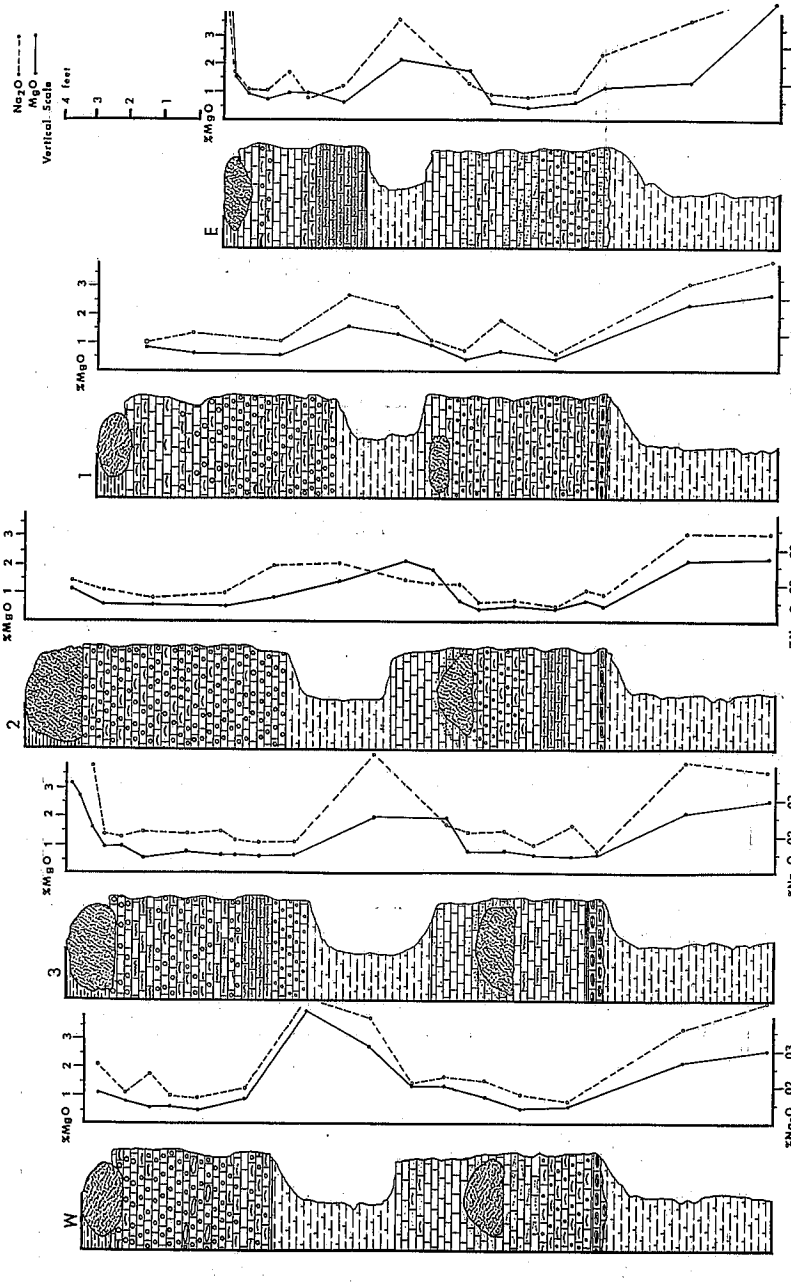

TEXT-FIGURE 7.—Na_2O (dashed) and MgO (solid) percentage plots for study sections.

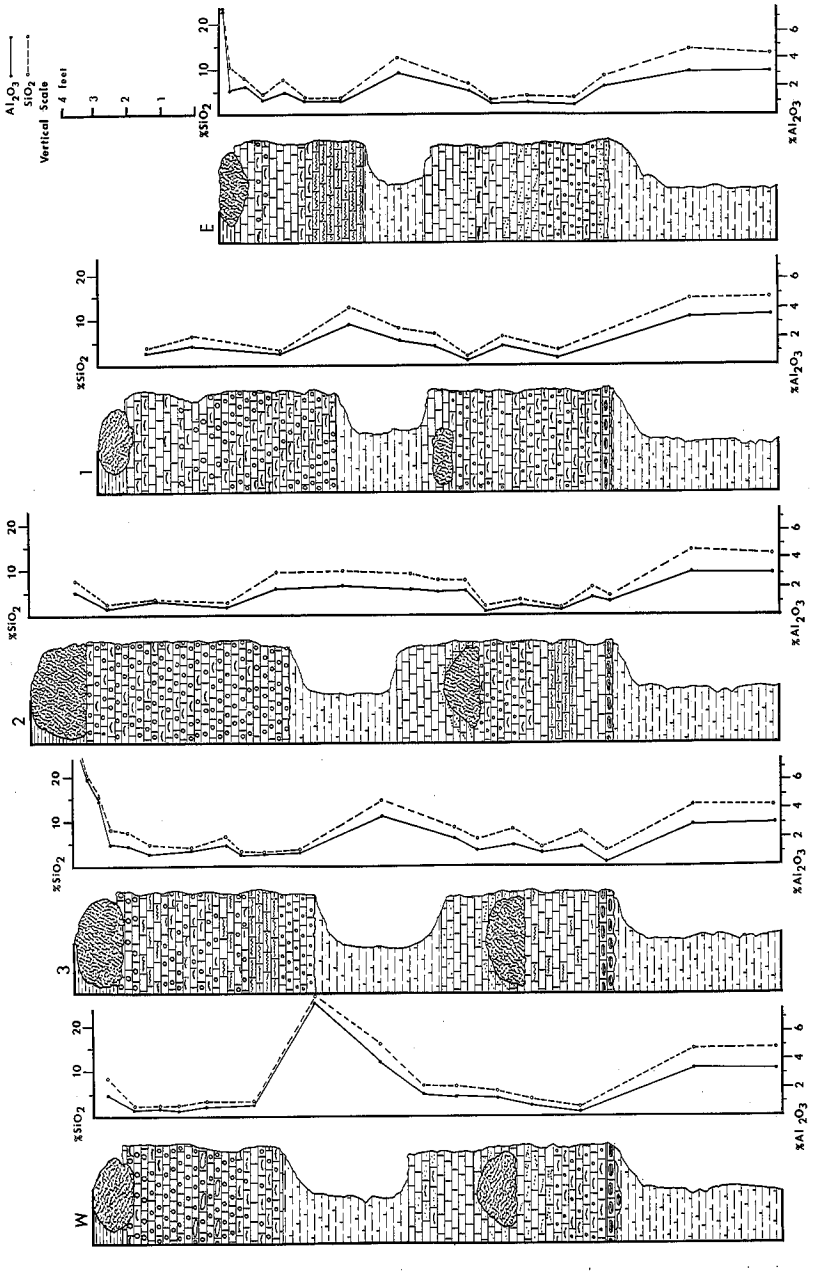

TEXT-FIGURE 8.—Al_2O_3 (solid) and SiO_2 (dashed) percentage plots for study sections.

plots proved inclusive and merely reflected the gross increase in SrO (Text-figures 9, 11).

A positive correlation, however, does exist between strontium and oolites in Unit A, and Goldsmith (1946) concluded that inorganic calcite may contain excessive amounts of strontium. This data strongly suggests that strontium is incorporated in the carbonate fraction as a cation in aragonite that occurs in the unit as oolites.

In summation, the total carbonate fraction reflects and substantiates the tripart division of a cycle. Calcium correlates negatively with the hydrolysate fraction of the cycle and magnesium correlates postively with the hydrolysate fraction.

Hydrolysates

Hydrolysates (clay minerals) occur in all units of both cycles. Aluminum, silicon, potassium, and sodium show a strong positive correlation (Text-figs. 8, 7, 6). Iron and magnesium (Text-fig. 10) correlate well with silicon and aluminum, but the correlation is not as pronounced as sodium and potassium's correlation. Welky (1952) stated that alkali metals, potassium, and sodium are associated with clay minerals. However, iron and magnesium may be incorporated in the sediments as carbonates. The increased iron and magnesium are possibly caused by temperature and salinity increases affecting carbonate formations during the influx of suspended hydrolysates into the depositional realm.

The amount of silica serves as an indicator of the relative amounts of aluminum; K_2O and NaO and varies, as expected, with the greatest weighted mean SiO_2 content (22.34) occurring in the green noncalcareous shales of Unit C, Cycle 2 (Table 1; Text-fig. 2). Progressively smaller amounts occur in the lower units of the cycles with Units B and C of Cycle 1 containing 8.58 and 3.77 percent SiO_2 respectively.

The increased abundance of the hydrolysate fraction in Units B and C versus Unit A has two environmental implications. First, progressive increase in the hydrolysate fraction in Units B and C may mean that a mechanism by which terrigenous sediments were transported to the depositional site became more effective during the deposition of Unit B and most effective during the deposition of Unit C. Another possible explanation for the clay increase might be the cessation of a process that acted as a deterrent to terrigenous transport into the depositional site.

Secondly, because algal bioherms occur in Units B and C the water depth in the region must have decreased during deposition of the units. Algae, requiring sunlight for photosynthetic processes, must by necessity be close to the surface in the muddy waters in order to receive sufficient sunlight. This conclusion is supported by the numerous desiccation features found in Unit B of both cycles.

In summation, it can be deduced from hydrolysate contents and other features that during the deposition of Unit A the waters were the deepest and most mud-free. During the deposition of Units B and C, the water depth decreased and mud content of the water increased.

Resistates

The resistate fraction in the various units of the cycles is negligible. Text-figure 8 shows that aluminum and silicon have a strong positive correlation in

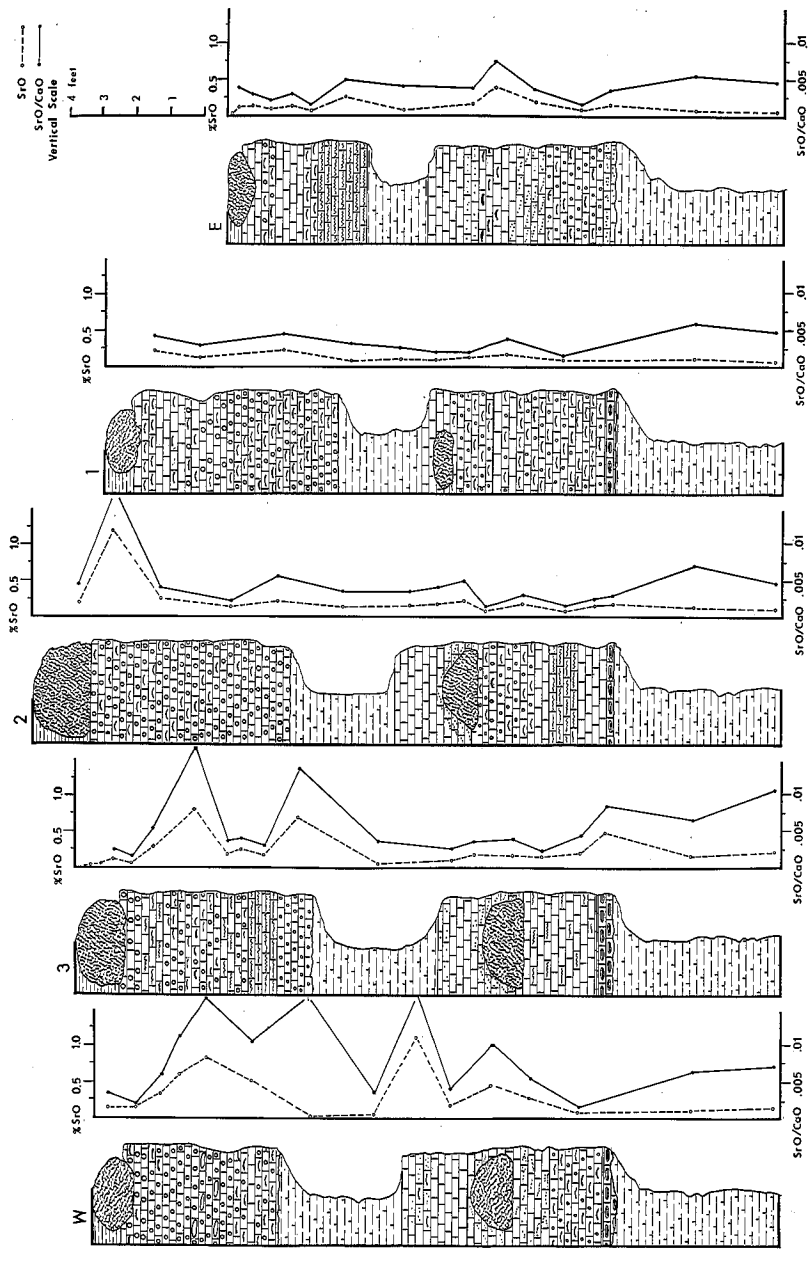

TEXT-FIGURE 9.—SrO (dashed) and SrO/CaO (solid) percentage and ratio plots for study sections.

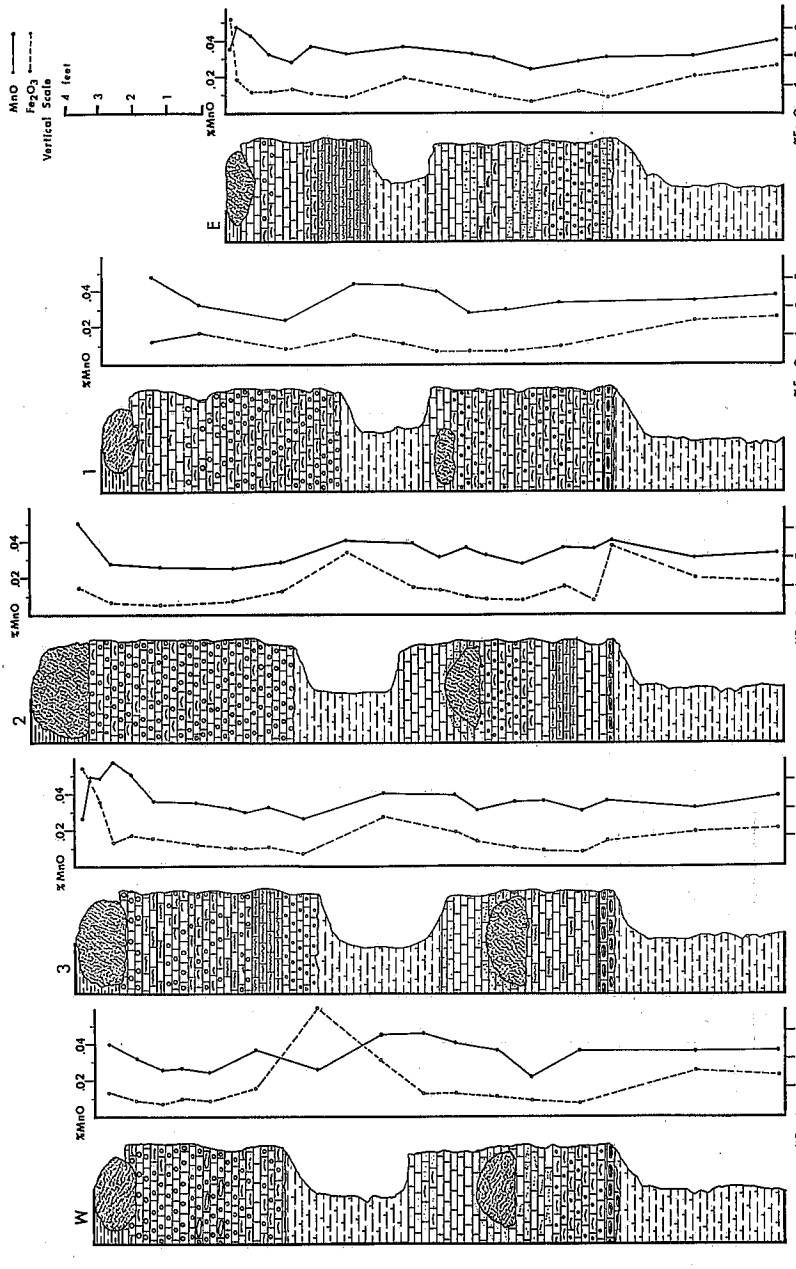

TEXT-FIGURE 10.—MnO (dashed) and Fe_2O_3 (solid) percentage plots for study sections.

all units of the cycle. This strong correlation is interpreted to mean that most silica occurs in a compound with aluminum. This observation, coupled with the lack of observable detrital quartz in 70 thins sections from the two cycles, is interpreted to mean that insignificant amounts of resistates are incorporated in the cycles.

The lack of significant resistates in the cycle cannot be interpreted to mean that water energy was too low to transport resistates to the depositional site because rounded rudite-sized autochthonous clastic grains are common, signifying vigorous water energy. Therefore, lack of resistates suggests that the depositional site was far removed from clastic source areas.

Oxidates

The contribution of oxidates to the total volume of rock in a cycle is unknown because of the lack of mineralogical data. Iron shows a strong positive correlation with aluminum and silicon (Text-figs. 8, 10) in the terrigenous calcisiltites of Unit C, and a positive correlation with magnesium in Units B and A (Text-fig. 7). This means that iron is not exclusively incorporated in association with clay minerals, but may be part of a carbonate.

Manganese, which could potentially form oxidate fractions in the rock, is most abundant in the algal bioherms of Unit B, Cycle 2. The greatest weighted mean percentage of MnO (.049) is found in the bioherms of Cycle 2 with none of the other units of the cycle containing more than .039 percent MnO. This may be interpreted to mean that organic activity was a factor in manganese extractions from the Virgin seas.

Manganese and iron exhibit a modest to fair positive correlation in all lithologies except the green shales of Unit C where they show a strong negative correlation. Baer (1965) cited work by Krauskopf (1957) and stated that a high Fe/Mn ratio should indicate oxidation, and a low ratio should indicate reducing conditions. A Fe/Mn plot was constructed, but in the absence of mineralogical data, conclusions based on the plot are indecisive (Text-fig. 11).

Evaporates

No evaporate minerals were observed in the outcrops, and the presence of calcium, sodium, potassium, and magnesium are accounted for as hydrolysates and carbonates. The evaporate fraction of a cycle is, therefore, taken to be nonexistent. This is not to state, however, that during the deposition of the cycles, evaporation of the Triassic waters was a significant factor in determining the relative elemental composition of hydrolysates and carbonates. To the contrary, evaporation during the deposition of Units B and C probably played a significant role in varying water temperature and salinity, thus concentrating various cations in the hydrolysate and carbonate fraction of the Virgin Limestone.

Summary

A critical overview of geochemical data shows that the greatest preponderance of the cyclic Virgin sediments were deposited as carbonates or hydrolysates. The two fractions are negatively correlated, with carbonate minerals comprising the dominant rock-forming portion during the deposition of Unit A. Hydrolysates gradually supplanted carbonates during the deposition of the cycle so that during the commencement of a cycle, CaO content dropped as low as .01 percent.

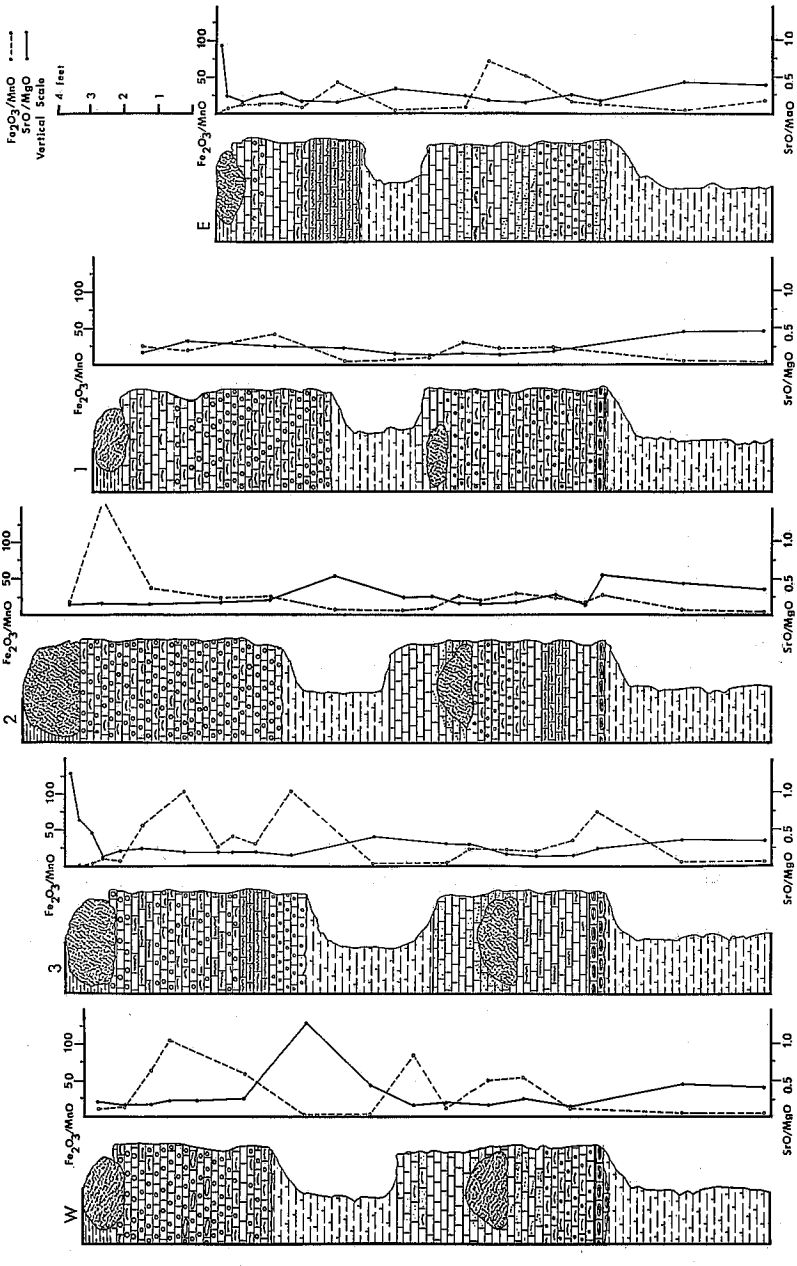

TEXT-FIGURE 11.—Fe_2O_3/MnO (dashed) and SrO/MgO (solid) ratios for study sections.

GEOCHEMICAL TRENDS

Lateral elemental variations in Units A of both cycles correlate well with the regional depositional picture and are significant in interpreting local depositonal parameters. These chemical trends may be used to determine shoreline location and proximity in similar sequences in the Triassic of southern Nevada and may have application in similar carbonates of other ages.

Calcium.—The amount of calcium in Unit A shows a positive correlation with unit thickness and mean grain percentage modified by a slight east to west increase in calcium. (Text-fig. 12).

Silicon.—Silicon shows a strong positive correlation with aluminum, sodium, potassium, and iron; thus any plot of silicon would be indicative of the hydrolysate fraction.

Silicon correlates negatively with unit thickness and weighted mean grain percentage with a slight east to west decrease in silicon matched to east to west increase in calcium (Text-fig. 12).

Strontium.—Silica and strontium show a strong negative correlation (Text-fig. 12), but strontium has no observable correlation with unit thickness and weighted mean grain percentage. The only positive correlation with strontium occurs in Unit A, Cycle 1, where corresponding increase in oolites and coated grain frequency was noted to parallel the corresponding east to west increase in SrO percentage.

Magnesium.—Magnesium is positively related to silicon and negatively associated with calcium in Sections E through 3. This correlation does not hold in Section W where magnesium shows a positive correlation with calcium and strontium (Text-fig. 12).

UNIT A, CYCLE 1

Calcium.—Calcium shows a strong positive correlation to unit thickness and weighted mean grain percentage, with a slight east to west calcium oxide increase similar to Unit A, Cycle 2 (Text-fig. 13).

Silicon.—Silicon has a strong negative correlation with calcium, unit thickness and weighted mean grain percentage and shows moderate east to west decrease in silica corresponding to the east to west increase in calcium (Text-fig. 13).

Strontium.—Strontium in Unit A of Cycle 1, unlike Cycle 2, is positively correlated with silica and magnesium and negatively associated to unit thickness with the exception of section W; however, the oolite density in Unit A was not studied because recrystallization made point count data uncertain.

Magnesium.—Magnesium shows the same positive correlation with silica in Cycle 1 as it did in Cycle 2 with a minor east to west elemental increase in magnesium.

Summary.—The depositional model formulated with petrologic data is supported and reaffirmed by geochemical trend data. Calcium's positive correlation with the thickness of Units A and the mean grain percent of the unit, and silicon's negative correlation with the same are expected results in carbonate bank deposits, where deposition of individual carbonate grain is the mechanism for

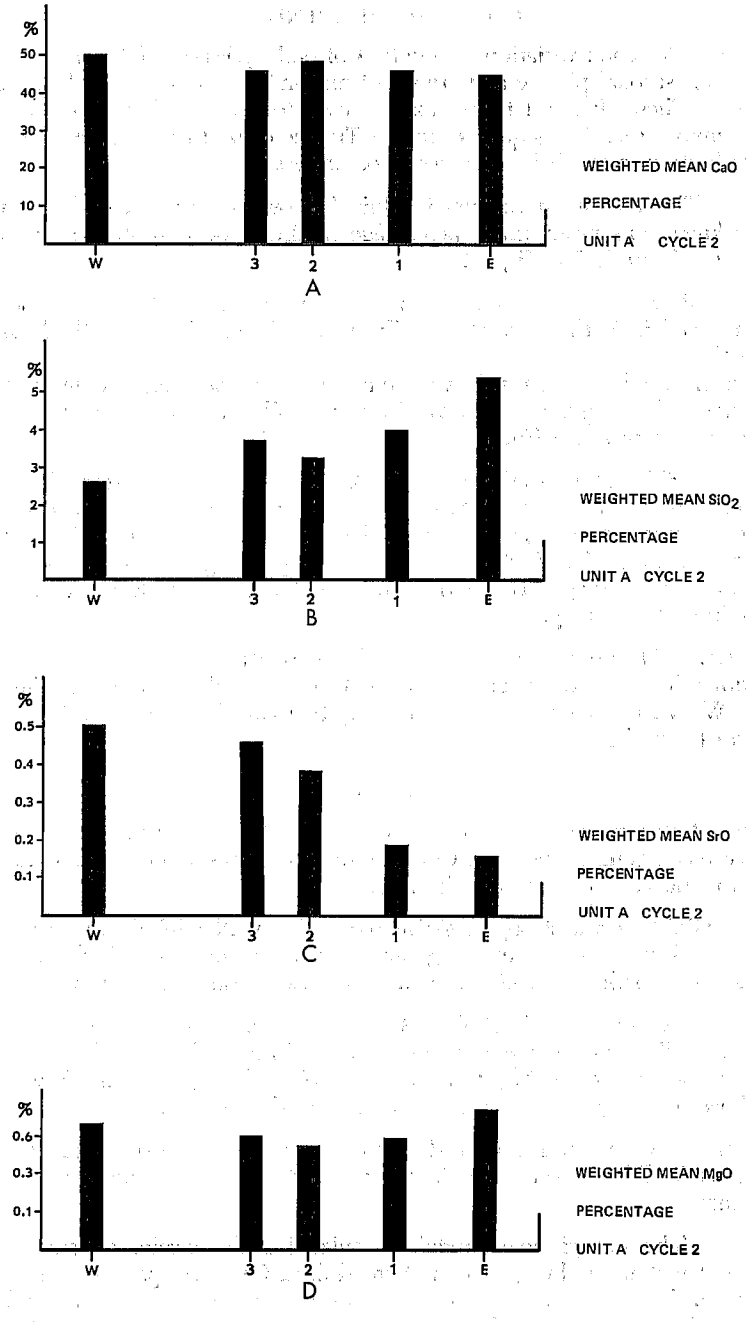

TEXT-FIGURE 12.—Histograms A, B, C, and D showing weighted mean CaO, SrO, SiO_2, and MgO percentages for Unit A, Cycle 2.

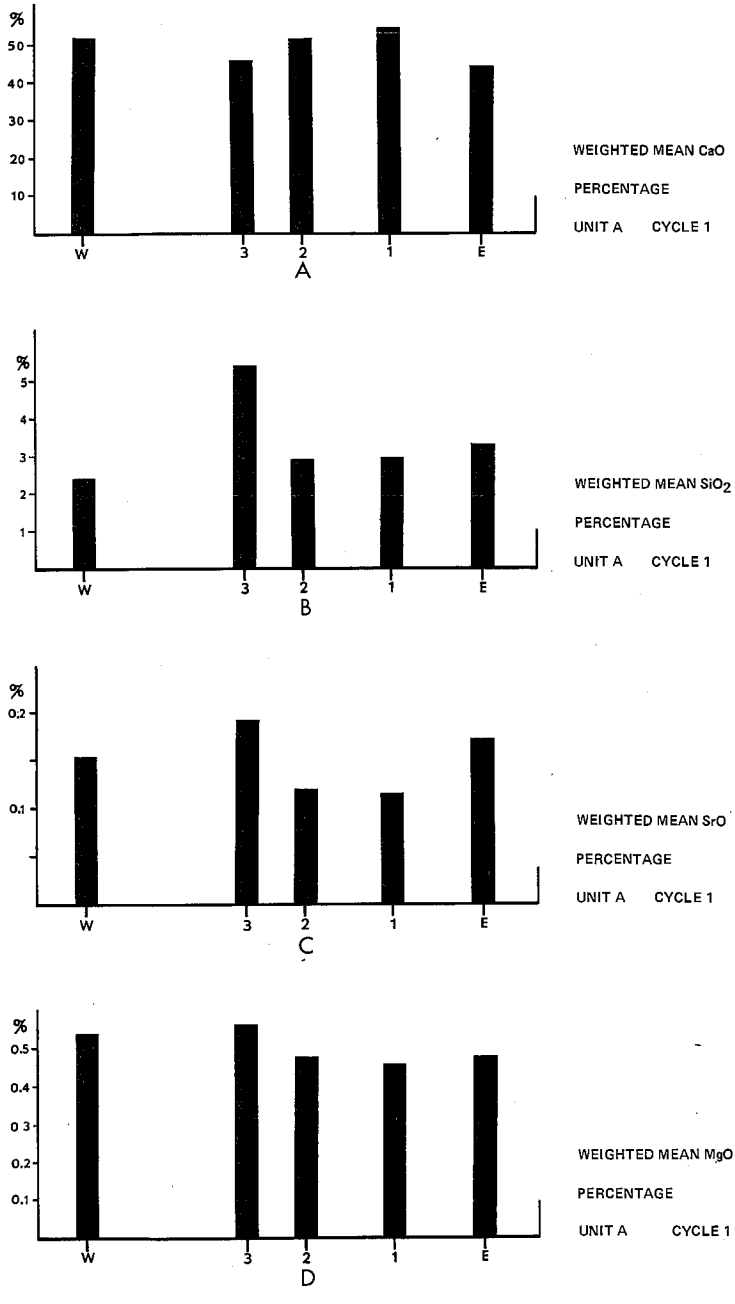

TEXT-FIGURE 13.—Histograms A, B, C, and D showing weighted mean CaO, SiO_2, SrO and MgO percentages for Unit A, Cycle 1.

deposition of the bank. Calcium contents should be high and silica contents low in the offshore position of the bank where vigorous water movements would winnow the sediments and deposit a carbonate-rich, hydrolysate-poor bank. Conversely, as the strandline is approached the hydrolysate fraction, represented by silica, should become a more important constituent of the bank sediments. Magnesium's west to east or offshore to onshore concentration increase is to be expected inasmuch as turbid, saline, warm near-shore waters should yield a carbonate rich in magnesium relative to the mud-free, cool offshore water that covers the outer portion of the bank.

The conclusions reached as the result of interpretations of geochemical data correspond to conclusions reached via petrologic methods. Therefore the question arises, if interpretations of petrologic data yields the same result as interpretation of geochemical data, why go to the time and expense to obtain geochemical data? Geochemical contributions to the study are threefold and significant in terms of position and qualitative measurements.

Primarily, geochemical data define the tri-part division of a cycle and enable one to divide the cycles in the absence of petrologic criteria, as in the case of Cycle 1, Section E (Text-figs. 6-11). Furthermore geochemical ratios could be used to provide quantitative measurements in terms of temperature and salinity with the addition of mineralogical and paleontological data but in the absence of this data ratios provide only relative quantity measurements.

Secondarily, later variations of elemental quantities which have important paleoenvironmental implications, such as magnesium, silica and calcium are revealed by geochemical data and are not noted in petrology data.

The third and possibly the most significant futuristic contribution that geochemistry makes to the study is that elemental trend relationships discovered may prove useful as a tool in subsurface carbonate exploration. Geochemical parameters, derived from well cuttings, which do not prove conclusive petrologic information, could be used in deposits similar to Virgin carbonate cycles to help locate carbonate banks and possibly associated biohermal masses.

CONCLUSIONS

Petrologic and geochemical data are extremely complementary and infer that marine transgressions and regressions are the mechanism by which carbonate cycles were deposited in the Virgin Member of the study area.

A west to east invasion of basinal marine waters over the tidal flat realm of the shelf produced a subaqueous erosional surface upon which inorganic carbonate grain banks were built by marine currents. The coarsest grained carbonates were found in the western portion of the bank where wave and current motion was the most vigorous, whereas the terrigenous matter was deposited more abundantly in the eastern or near-shore portion of the bank.

As the sea regressed, deposition of carbonate bank materials ceased and algal communities grew on the bank, and trapped magnesium-rich, fine-grained carbonates produced in the warm shallow waters of the realm.

Growth of the algal communities was terminated by an increase in the turbidity of the water which filtered out sunlight essential to bioherm growth, and the deposition of rock types characteristic of Unit B ceased.

Deposition of carbonate-poor terrigenous calcisiltites characteristic of the tidal flat environment on the shelf during early Triassic time resumed in the

area until such time as subsequent invasions of miogeosynclinal waters produced other carbonate cycles.

ECONOMIC IMPLICATIONS

The algal bioherms of Unit B and the carbonate banks of Unit A are potential hydrocarbon reservoirs. Both rock types emit hydrocarbon odors when broken, and porous portions of the algal bioherms commonly contain bituminous residues. Shell Oil Company's Bowl of Fire #1 well, approximately 15 miles northeast of the study area, had fair to excellent shows of oil in the limestones of the Virgin Member. Bissell (1968) referred to small bioherms in the Rainbow Garden area east of Las Vegas, Nevada, that bleed oil after being broken and exposed to the sun's heat for a few hours.

These occurrences serve to prove the presence of hydrocarbons in the limestone facies of the Virgin Member. The writer is of the opinion that significant quantities of oil could be extracted from the banks and algal bioherms of the carbonate cycles in the Virgin Limestone of southeast Nevada. The two cycles studied are not thick enough to contain banks of sufficient size to serve as reservoirs. The bioherms are small and isolated by fine-grained carbonate bodies. However, large cycles found in the upper part of the Virgin contain banks several tens of feet thick and bioherms could coalesce and form masses large enough to pool economic quantities of oil nearer the Las Vegas Line. Furthermore, geochemical parameters outlined in the study integrated with petrologic information could prove useful in the location of both reservoir types in the subcrop in the event of exploratory ventures in the region.

APPENDIX 1

Percentage Chemical Composition of Analysed Samples

Sample No.	SiO_2	Al_2O_3	Fe_2O_3	MnO	CaO	SrO	MgO	Na_2O	K_2O
EA	14.37	3.10	1.32	0.031	15.75	0.090	1.33	0.054	2.021
EB	13.85	3.12	1.57	0.040	17.25	0.080	4.20	0.063	1.812
E1	8.35	1.95	0.58	0.030	40.50	0.150	1.13	0.035	0.765
E2	3.80	0.65	0.77	0.028	52.00	0.095	0.60	0.014	0.112
E3B	3.95	0.78	0.35	0.024	51.50	0.190	0.38	0.011	0.247
E3U	3.07	0.70	0.57	0.030	51.00	0.390	0.55	0.013	0.221
E4	6.74	1.60	0.75	0.032	41.25	0.150	1.70	0.019	0.546
E6	12.58	2.85	1.24	0.036	21.25	0.085	2.13	0.054	1.370
E7	3.37	0.87	0.52	0.033	52.50	0.265	0.60	0.017	0.276
E8	3.50	0.95	0.69	0.036	48.50	0.085	0.93	0.011	0.276
E9	7.82	1.48	0.83	0.028	39.75	0.120	0.90	0.025	0.608
E10	4.65	1.00	0.76	0.033	46.25	0.100	0.70	0.015	0.358
E11	7.96	1.95	0.73	0.043	42.83	0.135	0.88	0.016	1.251
E11B	10.09	1.74	1.16	0.047	30.75	0.120	1.50	0.025	0.745
ABY	23.04	7.43	3.31	0.035	1.00	0.020	5.20	0.074	6.064
1A	14.40	3.25	1.56	0.035	16.75	0.100	2.30	0.047	1.520
1B	14.59	3.43	1.63	0.038	15.75	0.075	2.68	0.059	1.714
1C	12.97	3.05	1.56	0.036	19.75	0.090	2.45	0.054	1.460
12	2.83	0.47	0.67	0.034	55.83	0.095	0.43	0.008	0.145
13	6.07	1.30	0.41	0.030	42.50	0.165	0.70	0.027	0.461
14	1.69	0.38	0.48	0.028	57.75	0.115	0.38	0.010	0.061
15L	6.49	1.35	0.49	0.040	42.25	0.090	0.90	0.016	0.031
15	8.13	1.70	0.73	0.044	35.25	0.095	1.30	0.034	0.655
15A	12.60	2.85	1.03	0.044	21.25	0.070	1.53	0.041	1.394
16	2.97	0.85	0.58	0.024	50.00	0.220	0.53	0.015	0.187
17	6.25	1.36	1.09	0.033	39.50	0.120	0.60	0.020	0.521
18	3.90	0.87	0.80	0.048	50.00	0.210	0.80	0.014	0.228
2A	14.05	3.00	1.31	0.031	18.00	0.130	2.08	0.048	1.390
2B	13.15	2.91	1.16	0.034	19.75	0.095	2.23	0.048	1.352
21	3.93	0.88	2.39	0.041	50.25	0.150	0.53	0.013	0.296
22	5.62	1.18	0.49	0.036	46.38	0.115	0.70	0.016	0.426
23	0.90	0.30	0.97	0.037	57.25	0.085	0.35	0.006	0.080
24	2.94	0.60	0.50	0.028	51.00	0.150	0.50	0.010	0.219
25	1.83	0.24	0.53	0.033	54.50	0.080	0.40	0.009	0.065
26B	7.78	1.74	0.63	0.037	38.75	0.190	0.70	0.019	0.528
26L	7.97	1.67	0.85	0.032	40.00	0.165	1.80	0.019	0.577
26S	8.93	1.83	0.97	0.039	34.00	0.130	2.10	0.022	0.717
27	9.44	1.98	2.19	0.041	31.50	0.110	1.43	0.031	0.864
28	9.19	1.80	0.58	0.028	33.50	0.190	0.78	0.029	0.760
29L	2.30	0.55	0.45	0.025	52.75	0.120	0.50	0.014	0.163
29H	2.52	0.95	0.38	0.026	51.75	0.205	0.55	0.012	0.215
210	2.05	0.47	0.43	0.028	51.25	1.380	0.55	0.016	0.141
211	7.85	1.57	0.92	0.050	39.50	0.185	1.05	0.021	0.435
3A	13.29	2.90	1.19	0.032	21.25	0.145	2.13	0.060	1.296
3B	13.28	2.90	1.30	0.038	18.83	0.200	2.53	0.054	1.350
3C	14.35	3.13	1.40	0.037	17.83	0.085	2.13	0.087	1.477
31	3.15	0.34	0.90	0.036	54.50	0.480	0.63	0.012	0.129
32A	7.48	1.29	0.50	0.030	39.25	0.190	0.55	0.025	0.623
32B	4.00	0.86	0.54	0.036	51.00	0.125	0.60	0.014	0.308
34B	8.03	1.44	0.65	0.035	41.25	0.170	0.75	0.022	0.470

APPENDIX 1 (Cont.)

Sample No.	SiO_2	Al_2O_3	Fe_2O_3	MnO	CaO	SrO	MgO	Na_2O	K_2O
34S	8.32	1.87	1.17	0.039	35.12	0.095	1.90	0.026	0.742
34C	5.70	1.13	0.89	0.030	47.00	0.170	0.75	0.021	0.404
35	14.28	3.50	1.72	0.040	16.50	0.060	1.95	0.065	1.570
36	3.28	0.90	0.41	0.026	49.50	0.680	0.58	0.016	0.216
37	2.27	0.80	0.66	0.032	52.50	0.160	0.55	0.016	0.147
38	2.90	0.78	0.60	0.029	53.00	0.225	0.58	0.017	0.227
39	6.21	1.37	0.61	0.031	44.75	0.165	0.60	0.022	0.485
310	3.81	1.03	0.73	0.034	47.38	0.790	0.70	0.020	0.355
311	4.42	0.87	0.97	0.036	51.00	0.280	0.50	0.022	0.278
312	7.23	1.30	1.03	0.050	39.50	0.070	0.93	0.018	0.468
313	8.15	1.47	0.82	0.058	37.13	0.105	0.90	0.020	0.467
314A	16.24	4.85	2.32	0.048	11.50	0.060	1.73	0.040	1.910
314B	21.64	6.05	3.02	0.049	6.25	0.055	2.75	0.061	3.420
314C	27.04	8.15	3.45	0.027	0.01	0.025	3.13	0.082	9.999
WA	14.65	3.35	1.60	0.036	15.75	0.100	2.13	0.051	1.600
WB	14.55	3.28	1.44	0.036	16.25	0.115	2.55	0.072	1.658
WC	13.50	3.05	1.28	0.040	19.50	0.105	1.95	0.053	1.505
W2	1.87	0.20	0.48	0.037	54.00	0.075	0.58	0.012	0.080
W3	3.27	0.70	0.52	0.022	50.25	0.270	0.50	0.015	0.195
W4B	5.50	1.18	0.70	0.037	42.75	0.450	0.90	0.023	0.380
W4M	6.23	1.30	0.81	0.041	41.25	0.165	1.28	0.025	0.527
W4T	6.58	1.55	0.81	0.046	38.50	1.080	1.28	0.021	0.635
W5L	15.75	3.80	1.96	0.045	13.50	0.050	2.65	0.057	1.770
W5U	26.45	8.02	3.38	0.026	0.09	0.010	3.93	0.079	9.999
W6	3.10	0.80	0.95	0.037	49.25	0.510	0.85	0.018	0.265
W7	3.04	0.65	0.53	0.024	50.25	0.840	0.48	0.013	0.180
W8L	2.02	0.41	0.62	0.027	56.00	0.610	0.58	0.014	0.147
W8H	2.03	0.50	0.46	0.026	54.00	0.330	0.53	0.026	0.159
W9	2.02	0.44	0.58	0.032	53.83	0.115	0.78	0.016	0.125
W10	8.25	1.46	0.85	0.040	36.63	0.125	1.05	0.032	0.434

REFERENCES CITED

Baer, J. L., 1969, Paleocology of cyclic sediments of the Lower Green River Formation, Central Utah: Brigham Young Univ. Geol. Studies, v. 16, pt. 1, p. 3-95.

Bissell, H. J., 1968, Permian and Lower Triassic transition from the shelf to basin (Grand Canyon, Arizona to Spring Mountains, Nevada): Four Corners Geol. Soc. Guidebook, Fifth Ann. Field Conf., 1969, p. 135-169.

Bissell, H. J., and G. V. Chilingar, 1968, Shelf-to-basin Permian sediments of southern Nevada, USA: International Geol. Congress, 23rd. session, Czechoslovakia, Proc. Sec. 8, p. 155-167.

Brimhall, W. H., and G. F. Embree, 1970, Rapid analysis of basalts by atomic absorption spectrophotometry: unpublished manuscript.

Clark, D. L., 1957, Marine Triassic stratigraphy in eastern Great Basin: Amer. Assoc. Petrol. Geol. Bull., v. 28, p. 61-74.

Chilingar, G. V., 1956, Use of Ca/Mg ratio of limestones and dolomites as a geologic tool: unpub. Ph.D. dissertation, Univ. of Southern Calif., 140 p.

Degens, E. T., 1965, Geochemistry of sediments: Prentice-Hall, Inc. 342 p.

Goldberg, E. D., 1957, Biogeochemistry of trace metals: Geol. Soc. Amer. Mem. 67, p. 345-357.

Graf, D. L., 1960, Geochemistry of carbonate sediments and sedimentary carbonate rocks: Illinois State Geol. Sur. Circular 308, 5 parts.

Krauskopf, K. B., 1957, Separation of manganese from iron in sedimentary processes: Geochem. Cosmochem. Acta, v. 12, p. 61-84.

Larsen, A. R., and N. G. Lane, 1964, Repetitive bedding in Triassic sediments in Clark County, Nevada: Kansas Geol. Surv. Bull. 169, v. 1, p. 39-62.

Lowenstam, H. A., 1954, O^{18}/O^{16} ratios and Sr and Mg contents of calcareous skeletons of Recent and fossil brachiopods and their bearing on the history of the oceans: Preprints of abstract, International Oceanographic Congress, 31 August-12 September, Amer. Assoc. Adv. Sci., Washington, D.C., 1959, p. 71-72.

Mason, B., 1966, Principles of geochemistry: John Wiley and Sons, Inc., 329 p.

Newell, N. D., Rigby, J. K. and others, 1951, Shoal-water geology and environments, Eastern Andros Island, Bahamas: Bull. Amer. Mus. of Nat. Hist., v. 97, Art. 1, 29 p.

Odum, H. T., 1950, Strontium biochemistry, ecosystems and paleoecological tools: Nat. Research Council Comm. Treatise Marine Ecology and Paleoecology, Rept. 1949-50, no. 10, p. 55-58.

Pilkey, O. H., and Howard J., 1960, The effect of environment on the concentrations of skeletal magnesium and strontium in *Dendraster*: Jour. Geol., v. 68, p. 203-216.

Poborski, S. J., 1954, Virgin Formation (Triassic) of the St. George, Utah, area: Geol. Soc. Amer. Bull., v. 65, p. 971-1006.

Reeside, J. B., and Bassler, H., 1922, Stratigraphic sections in southwestern Utah and northwestern Arizona: U.S. Geol. Survey Prof. Paper 129, p. 52-77.

Sander, N. J., 1967, Classification of carbonate rocks of marine origin: Amer. Assoc. Petrol. Geol. Bull., v. 53, p. 325-336.

Sanderson, I. D., 1967, Lithology and petrography of the Virgin Limestone (Lower Triassic) at Blue Diamond Hill and vicinity, Clark County, Nevada: Brigham Young Univ. Geol. Studies, v. 14, p. 123-130.

Siegel, F. R., 1961, Variations of Sr/Ca ratios and Mg contents in recent carbonate sediments of northern Florida Keys area: Jour. Sed. Petrol., v. 31, no. 3, p. 336-342.

Turekian, K., 1955, Paleoecologic significance of the Strontium-calcium ratio in fossils and sediments: Bull. Geol. Soc. Amer. v. 66, p. 155-158.

Welby, C. W., 1952, The occurrence of the alkali metals in some modern sediments: unpub. Ph.D. dissertation, Massachusetts Institute Tech.

Welby, C. W., 1958, Occurrence of alkali metals in some Gulf of Mexico sediments: Jour. Sed. Petrol., v. 28, p. 431-452.

Manuscript received October 5, 1970